



# 1 **Forest Diversity and Environmental Factors Shape Contrasting** 2 **Soil-Litter BVOC and Methane Fluxes in Three Central** 3 **Amazonian Ecosystems**

4 Débora Pinheiro-Oliveira<sup>1\*</sup>, Hella van Asperen<sup>2,3</sup>, Murielli Garcia Caetano<sup>4</sup>, Michelle Robin<sup>2</sup>,  
5 Achim Edtbauer<sup>5</sup>, Nora Zannoni<sup>6</sup>, Joseph Byron<sup>5</sup>, Jonathan Williams<sup>5</sup>, Layon Oreste Demarchi<sup>7</sup>,  
6 Maria Teresa Fernandez Piedade<sup>7</sup>, Jochen Schöngart<sup>7</sup>, Florian Wittmann<sup>8</sup>, Sergio Duvoisin-  
7 Junior<sup>9</sup>, Carla Batista<sup>9</sup>, Rodrigo Augusto Ferreira de Souza<sup>10</sup>, Eliane Gomes Alves<sup>2,1\*</sup>

8 <sup>1</sup> Graduate Program in Climate and Environment, National Institute for Amazonian Research, Manaus, Brazil

9 <sup>2</sup> Department of Biogeochemical Processes, Max Planck Institute for Biogeochemistry, Jena, Germany

10 <sup>3</sup> Institute for Environmental Physics, University of Bremen, Bremen, Germany

11 <sup>4</sup> Graduate Program in Tropical Forest Sciences, National Institute for Amazonian Research, Manaus, Brazil

12 <sup>5</sup> Atmospheric Chemistry Department, Max Planck Institute for Chemistry, Mainz, Germany

13 <sup>6</sup> Institute of Atmospheric Sciences and Climate, National Research Council (CNR-ISAC), Bologna, Italy

14 <sup>7</sup> Coordination of Environmental Dynamics, National Institute of Amazonian Research, Manaus, Brazil

15 <sup>8</sup> Department of Wetland Ecology, Karlsruhe Institute of Technology, Rastatt, Germany

16 <sup>9</sup> Department of Chemistry, Amazonas State University, Manaus, Brazil

17 <sup>10</sup> Department of Meteorology, Amazonas State University, Manaus, Brazil

18 <sup>\*</sup>Correspondence to: Débora Pinheiro Oliveira ([dpinheiro@bgc-jena.mpg.de](mailto:dpinheiro@bgc-jena.mpg.de)); Eliane Gomes Alves ([egomes@bgc-](mailto:egomes@bgc-jena.mpg.de)  
19 [jena.mpg.de](mailto:egomes@bgc-jena.mpg.de))

## 20 **Abstract**

21 Biogenic volatile organic compounds (BVOCs) play a crucial role in biosphere-atmosphere  
22 interactions and the global carbon cycle. While vegetation is recognized as the primary source of  
23 BVOC fluxes in forest ecosystems, recent studies suggest that the carbon-rich soil-litter  
24 compartment contributes significantly. However, these fluxes, their underlying drivers, and their  
25 variability across forest types remain poorly understood, with measurements still scarce—  
26 particularly in the Amazon rainforest, the world’s largest source of BVOCs. In this study, we  
27 investigated soil-litter BVOC and methane fluxes and their potential drivers—including nutrient  
28 content, microbial biomass, soil temperature and moisture—across three forest types in central  
29 Amazonia: white sand forest (WS), upland forest (UP), and ancient river terrace forest (AR). Our  
30 results showed distinct flux patterns among forest types. WS exhibited both high emissions and



31 consumption of gases, notably high acetaldehyde and methane emissions, and strong isoprene and  
32 monoterpene uptake. UP showed lower overall fluxes, with moderate emission and consumption  
33 of DMS, isoprene, and acetaldehyde. AR presented no significant fluxes. Linear models identified  
34 soil moisture and temperature as the primary drivers of fluxes in WS, while microbial biomass was  
35 the main driver in UP. Our measurements suggest that, despite covering a relatively small area in  
36 the Amazon basin, WS can be a significant ecosystem for BVOC and methane fluxes, regulated  
37 by soil moisture and temperature. Our findings underscore the need to account for forest-type-  
38 specific fluxes when modeling BVOC and methane emissions in the Amazon, particularly under  
39 changing climate conditions.

#### 40 **Key words**

41 Amazon rainforest; Biogenic volatile organic compounds (BVOC); Methane (CH<sub>4</sub>); rain-induced  
42 emissions; Soil-litter fluxes; Forest heterogeneity; Soil-litter microorganism

#### 43 **1. Introduction**

44 Soil and litter constitute an ecological compartment that plays a crucial role in gas fluxes  
45 of biogenic volatile organic compounds (BVOCs) (Peñuelas et al., 2014; Tang et al., 2019) and  
46 greenhouse gases (GHGs) (Fan et al., 2020, 2024). Biological and physical processes are essential  
47 in soil and litter BVOC and GHG fluxes. In terms of biological processes, roots release BVOCs  
48 for communication, defense against herbivory and symbiotic relationships (Gfeller et al., 2013;  
49 Lin et al., 2007; Rasheed et al., 2021; Steeghs et al., 2004; Tang et al., 2019; Trowbridge et al.,  
50 2020), and soil microorganisms produce BVOCs for communication and ecological interactions  
51 (e.g., defense and competition), with these compounds also being released as residual metabolic  
52 products (Isidorov & Jdanova, 2002; Leff & Fierer, 2008; Liu et al., 2024; Monard et al., 2021).  
53 GHGs, such as methane (CH<sub>4</sub>) and carbon dioxide (CO<sub>2</sub>), are produced by microorganisms in the  
54 soil. Methane fluxes are primarily driven by methanogenic (archaea) and methanotrophic  
55 microorganisms in anaerobic and aerobic environments, contributing to the global methane budget  
56 (Conrad, 2009; Hofmann et al., 2016). The decomposition of litter also influences BVOC and  
57 GHG fluxes; particularly physical factors, such as temperature and soil moisture, greatly impact  
58 litter decomposition by influencing the activity of microorganisms, a process that also releases  
59 BVOCs and GHGs (Greenberg et al., 2012; Tang et al., 2019; Mäki et al., 2017; Asensio et al.,



60 2008). Temperature directly affects gas production and consumption (Conrad, 2009), the  
61 evaporation of stored compounds (Aaltonen et al., 2011), and the desorption from leaf litter tissue  
62 and soil organic matter (Bachy et al., 2018; Schade & Goldstein, 2001; Tang et al., 2019, Warneke  
63 et al., 1999). Soil moisture affects microbial activity (Abis et al., 2020; Liu et al., 2024) and BVOC  
64 adsorption (Jiao et al., 2023), thereby directly affecting the magnitude of soil gas fluxes (Conrad,  
65 2009; Liu et al., 2024; Pugliese et al., 2023; Shah et al., 2024; Svendsen et al., 2016). In addition  
66 to changes in soil moisture, precipitation events can induce BVOC emissions, e.g., by pushing  
67 stored soil BVOC gases out of the soil pore space (Miyama et al., 2020).

68 Soil type can also influence gas fluxes, with sandy soils facilitating BVOC volatilization  
69 and retention due to larger pore spaces that promote water movement and faster evaporation under  
70 higher temperatures (Onwuka, 2018). For example, soil texture influences the relationship between  
71 methane and soil moisture, with methane emission fluxes being generally higher in sandy soils  
72 than in clay soils (Cai et al., 1999), probably due to their larger pore size, which facilitates gas  
73 diffusion (Rosace et al., 2020). Additionally, changes in vegetation cover also impacts gas fluxes  
74 (Gomes Alves et al., 2022). Plant species composition influences BVOC emissions in terms of  
75 chemical composition and emission rates (Bao et al., 2023; Mu et al., 2022; Zhang et al., 2024),  
76 and since different soil types often support distinct vegetation (Rodrigues et al., 2018), soil-litter  
77 gas fluxes are expected to vary across forest types (Wachiye et al., 2020).

78 The Amazon basin is the largest source of BVOCs to the global atmosphere (Guenther et  
79 al., 2012). BVOCs are crucial for understanding climate dynamics due to their role in atmospheric  
80 chemistry. They contribute to the formation of secondary organic aerosols (SOAs) and influence  
81 cloud properties, which in turn affect global climate patterns (Fuentes et al., 2000; Jimenez et al.,  
82 2009). Although vegetation is considered the main source of these compounds, with large effects  
83 on the above-mentioned atmospheric processes, some studies have shown that soils are as  
84 important as plants for BVOC emissions (Penuelas et al., 2014).

85 The Amazon basin has different soil types (Quesada et al., 2011), which determine forest  
86 structure (Quesada et al., 2012) and plant species composition (Ter Steege et al., 2013), resulting  
87 in a mosaic of different forest types throughout the basin (Oliveira-Filho et al., 2020). These  
88 different forest and soil types have been little - or not at all investigated for soil-litter BVOC and



GHG fluxes and, therefore, are not included in model estimates. In this sense, studies integrating biological and physical measurements are essential to understand the processes controlling soil-litter BVOC and GHG fluxes across Amazonian forest types. Quantifying BVOC emissions from soil is essential for accurately modeling these processes and predicting their effect on climate, as soil can be a significant source of BVOCs.

With a unique set of measurements, we investigated soil-litter BVOC (acetaldehyde, methanol,  $m/z$  42, dimethyl sulfide, isoprene and monoterpenes) and GHG ( $\text{CH}_4$  and  $\text{CO}_2$ ) fluxes, soil and litter nutrient content and microbial biomass, and soil temperature and moisture from three forest types in central Amazonia: (i) ancient river terrace forest - a forest that was flooded in the past and is no longer flooded due to changes in the river course (paleoigapó); (ii) white sand forest (locally called *campinarana*) - a less common forest type that occupies about 5% of the Amazon basin (Adeney et al., 2016); and (iii) upland forest (locally called terra-firme) - the most common forest in Amazonia, with the highest plant species richness (Emidio et al., 2016; Luize et al., 2018). We aimed to answer the following questions: (i) what is the emission/consumption of gases (BVOCs,  $\text{CO}_2$ , and  $\text{CH}_4$ ) in magnitude and chemical diversity, and?; and (ii) what are the main drivers of soil-litter gas fluxes across these three forest types in central Amazonia?

## 2. Material and Methods

### 2.1 Site Description

This study was conducted in the MAUA–PELD experimental plots (PELD is the abbreviation in Portuguese for long-term ecological research) (Fig.1) at the Amazon Tall Tower Observatory (ATTO) experimental site. This site is located 150 km northeast of Manaus and is part of the Uatumã Sustainable Reserve (USDR), which covers an area of 424,430 hectares (Andreae et al., 2015). The climate is tropical humid, with average annual rainfall of 2,376 mm and a temperature of  $28^\circ\text{C}$  (Botía et al., 2022). There are two distinct seasons, the wet season from December to May and the dry season from July to October, with transition seasons in between. The ATTO site contains three dominant non-flooded ecosystems: a dense upland forest on the plateau, with an elevation close to 100 m (*terra-firme*); a white sand forest (*campinarana*); and another type of *terra-firme* vegetation that developed on the lower-laying ancient river terraces (ancient river terrace forests) (Fig. 1) (Andreae et al., 2015).

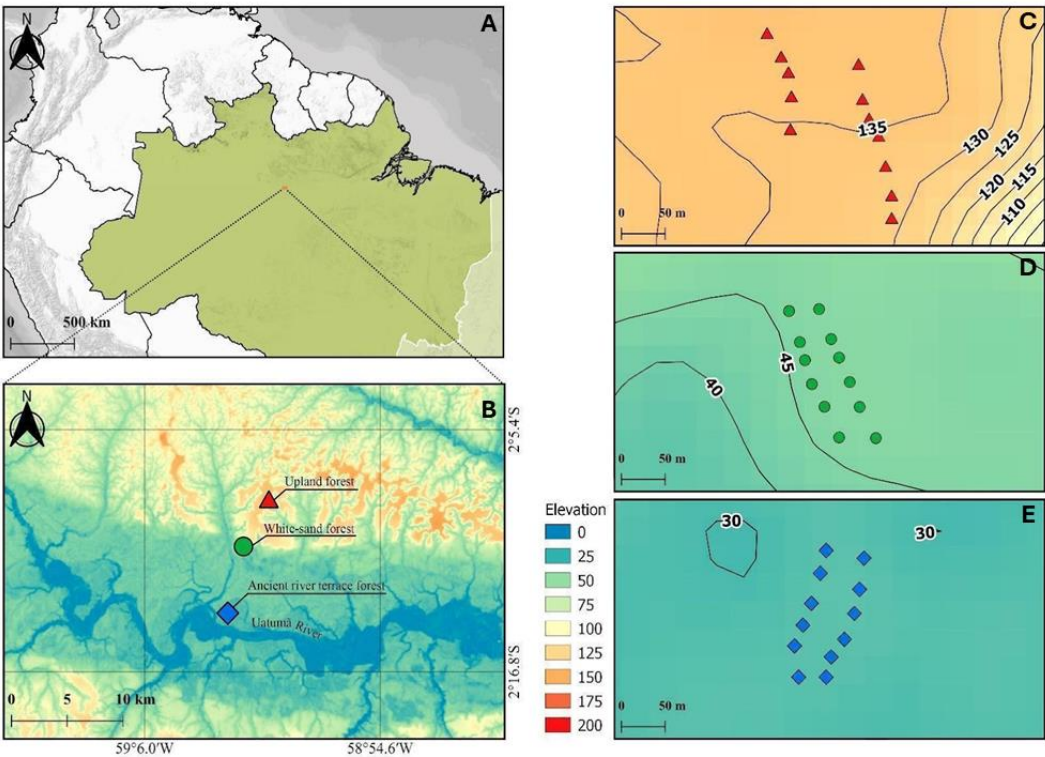


**Figure 1.** (A) Location of the ATTO site. (B) A map illustrating the locations of the different forest types evaluated in this study: upland forest, white sand forest, and ancient river terrace forest; and showing the Uatuma River, a tributary of the Amazon River. (C), (D) and (E): The distribution of sampling points along the transects in each forest type (upland forest - top, white sand forest - middle, and ancient river terrace forest - bottom); black lines and numbers indicate the elevation (above sea level – a.s.l.).

Topography is critical to soil formation in the central Amazon region (Quesada et al., 2009). At the ATTO site, a clear topographic gradient is associated with different soil characteristics (Fig. 1). In the ancient river terrace forest, soil contains more silt and clay (39% sand, 37% silt, 23% clay) in comparison to the adjacent sandy white sand forest soils (57% sand, 40% silt, 1.50% clay). Upland forest soils are more clayey and contain very little sand (13% total sand, 34% silt, 52% clay) (data from this study; supplementary material, Table S1). Upland forest soils, which are predominantly ferrasols, are known to hold more water than other tropical soils, benefiting forest



132 activity during the dry season (Quesada et al., 2009). Ancient river terrace forest soils are typically  
133 allisols, younger and richer in nutrients compared to upland ferralsols (Andreae et al., 2015). White  
134 sand forest soils are arenosols, characterized by high permeability and low water retention, with  
135 low specific heat capacity and often nutrient-poor organic layers (Quesada et al., 2011). The study  
136 area in the white sand forest has high water table variability, with a hard subsoil layer that restricts  
137 drainage and can flood the root system during the wet season (Demarchi et al., 2022).

## 138 **2.2 Sampling Design**

139 For each forest type, a PELD-MAUA plot (~1 hectare) was selected, wherein two 150 m transects  
140 were marked. Six collection points, approximately 30 m apart, were determined for each transect,  
141 resulting in a total of 36 soil chamber measurements (Fig. 1). Additionally, three blank chambers  
142 per transect were measured, which consisted of chambers with the same volume but with a  
143 completely bottom-sealed collar. These blank chambers were measured simultaneously and under  
144 the same conditions as the sample chambers covering soil and litter (Fig. 2b).

145 After each gas flux measurement, soil temperature (T, °C) (TP-101, Delhi, India) and soil  
146 volumetric water content (VWC, %) (AT SMT150, Cambridge, UK) were measured around the  
147 collar five times, and the average was calculated. Samples from the litter and surface soil layers  
148 were collected inside the chamber and stored for analysis of chemical and physical characteristics  
149 and microbial biomass. Due to expected low variation and limited possibility for laboratory  
150 analyses, nutrient samples from soil and litter (excluding carbon and nitrogen) and soil  
151 granulometry were collected as mixed samples from two collars. To minimize diurnal variation,  
152 each transect was measured between 8:00 and 10:00 (local time), after which collected bag samples  
153 were processed and analyzed for BVOC and GHG concentrations. During the measurements, no  
154 precipitation was observed, but one large rain event occurred just before the measurement of  
155 transect 2 of the white sand forest.

156

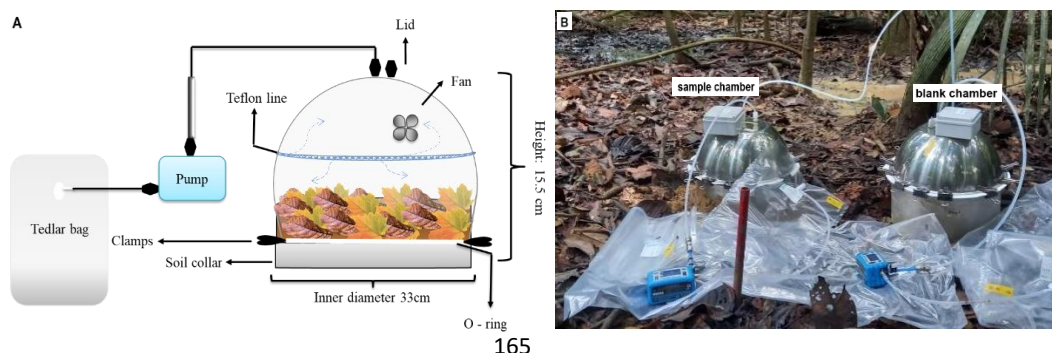
## 157 **2.3 Flux Chamber Measurements**

158 The flux chambers used in this study were produced by the Max Planck Institute for  
159 Biogeochemistry and were made of 100% stainless steel (Fig. 2), with a total volume of 21 L and  
160 a surface area of 855 cm<sup>2</sup> (0.0855 m<sup>2</sup>). Two Teflon inlets were connected to the top of the chamber,





161 and inside the chamber was a fan that provided air mixing of the gases in the chamber headspace.  
162 A PTFE-coated Viton O-ring was positioned at the edge of the collar over which the chamber was  
163 placed. The collar and the chamber were sealed together with multiple clamps to prevent outside  
164 air from entering the chamber.



166 **Figure 2.** (A) Schematic of the flux chamber. (B) Photo of the measurement setup of the sample  
167 and the blank chambers.

168 Before gas sampling, each soil collar was carefully installed in a non-invasive manner by gently  
169 pressing the collar edge into the soil to avoid damage to plant shoots and roots, and then sealed  
170 with the surrounding soil (Aaltonen et al., 2011). The collars were installed approximately 24 hours  
171 before the measurements.

## 172 2.4 Field gas measurements

173 The gas collection took place in December 2021, at the dry-to-wet season transition. Tedlar bags  
174 (CEL Scientific, Cerritos, CA, USA) were used to sample soil-litter gas fluxes (BVOCs, CO<sub>2</sub>,  
175 CH<sub>4</sub>). An air sampling pump (GilAir® Plus, Levitt Safety, Ottawa, ON) operated at a flow rate of  
176 500 sccm, ensuring continuous flow at the chamber outlet. After 20 minutes of chamber closure  
177 with continuous flow, a sampling bag was connected to the outlet of the Teflon pump, and a 5 L  
178 sample was collected over 10 minutes. At the end of the 30-minute process, a total of 15 L of air  
179 had flown through the chamber, of which the last 5 L was used for analysis by the PTR-QMS, the  
180 Los Gatos analyzer, and for collecting a cartridge sample (see below). For logistical reasons,  
181 measurements were conducted with three chambers at a time, pairing two sample chambers with  
182 one blank chamber, followed by two additional sets, resulting in measurements of six samples and  
183 three blank chambers per day.



184 Before placing the lid on the collar, the chamber was manually ventilated to minimize collar-  
185 induced CO<sub>2</sub> accumulation. The chamber was then closed, the internal fan was turned on, and the  
186 lid was sealed with clamps. Because air was continuously extracted from the chamber headspace,  
187 both (blank and sample) chambers had an attached 2 m long open Teflon tube, fixed approximately  
188 2 m above the ground and at the same location, which ensured that both chambers were diluted or  
189 affected by ambient air to the same degree. After collection, the bags were stored in a dark box for  
190 transport to the laboratory. Gas concentration analyses were conducted on the same day; first, the  
191 bags were measured using proton-transfer-reaction quadrupole mass spectrometry (PTR-QMS,  
192 IONICON Analytik, Innsbruck, Austria), followed by a Los Gatos Analyzer (see section 2.5).  
193 Subsequently, each bag was sampled using a cartridge (stainless steel tubes filled with Tenax TA  
194 and Carbograph 5 TD adsorbents) to be later qualitatively analyzed through thermal-desorption  
195 gas chromatography time-of-flight mass spectrometry (TD-GC-TOF-MS; Bench ToF Tandem  
196 Ionisation, Markes International, Bridgend, UK). To maintain conciseness and ensure clarity of  
197 our main findings, detailed descriptions of the analyses and results are presented in the  
198 supplementary material, sections 3 and 3.1. The Tedlar bags were analyzed or sampled within 10  
199 hours of analysis, as recommended by Beauchamp et al. (2024).

200

## 201 **2.5 PTR-QMS measurements and Los Gatos analyzer measurements**

202 Tedlar bags were connected to the PTR-QMS (Ionicon Analytik, Austria) for analysis of BVOC  
203 (Lindinger et al., 1998). The PTR-QMS H<sub>3</sub>O<sup>+</sup> mode was used for chemical ionization, which is  
204 extremely sensitive to all BVOCs that have a higher proton affinity than water, covering most  
205 volatile organic compounds (Edtbauer et al., 2021). Seven compounds were analyzed (Table 1).  
206 The PTR-QMS was operated under standard conditions at 2.3 mbar, and E/N 120, with 60°C, with  
207 a drift tube voltage of 600 V. During each PTR-QMS measurement cycle, the following specific  
208 protonated mass-to-charge ratios (m/z) were measured, 21 (H<sub>3</sub>O<sup>18+</sup>), 32 (O<sub>2</sub><sup>+</sup>), and 37 (H<sub>2</sub>O-  
209 H<sub>3</sub>O<sup>+</sup>), with a dwell time of 500 ms each; and Methanol (33), compound not identified (m/z 42),  
210 Acetaldehyde (45), Dimethyl sulfide (63), Isoprene (69) and Monoterpenes (137), with a dwell  
211 time of 1 second. We measured approximately 17 cycles for each bag. Mass identifications were  
212 based on the available literature (Warneke et al., 2015), and were consistent with a PTR-MS mass





library database - GLOVOC (Yañez-Serrano et al., 2021) and gas calibration with certified standards.

**Table 1.** Compounds analyzed by the PTR-QMS

| BVOC             | Chemical formula (H+)             | m/z | Group          |
|------------------|-----------------------------------|-----|----------------|
| Methanol         | CH <sub>4</sub> O+                | 33  | Alcohol        |
| not identified   |                                   | 42  | N-compound     |
| Acetaldehyde     | C <sub>2</sub> H <sub>4</sub> O+  | 45  | Aldehyde       |
| Isoprene         | C <sub>5</sub> H <sub>8</sub> +   | 69  | Alkenes        |
| Dimethyl sulfide | C <sub>2</sub> H <sub>6</sub> S+  | 63  | Organosulfides |
| Monoterpenes     | C <sub>15</sub> H <sub>16</sub> + | 137 | Alkenes        |

Calibrations were performed before the experiment using a multi-component calibration mix containing various known concentrations (supplementary material; Table S2) (Apel-Riemer Environmental, Inc.). Four-point calibration curves were generated by diluting the multicomponent with synthetic air, humidifying the air stream with a water bubbler filled with distilled water, and controlling the flow with mass flow controllers (0, 1, 3, and 5 ppb) (supplementary material; Fig. S1). Curves were calculated considering the normalized counts per second as a function of the mixing ratio. Previously, some compounds important for soil-litter processes (Peñuelas et al., 2014), - such as acetone, ethanol, and formaldehyde - were considered for this study, but they did not show a good fit, they were excluded from this work.

The mass m/z 42 can be attributed to acetonitrile; however, acetonitrile is usually considered a biomass-burning tracer/or, more generally, a compound of anthropogenic origin (Huangfu et al., 2021). Acetonitrile can be produced in the oceans (Sanhueza et al., 2004) and can also be consumed by these ecosystems. It can be produced by microorganisms (Raio et al., 2020), but there is a lack of evidence to support its emission from the soil. When using the PTR-QMS to measure m/z 42, it is essential to consider the possibility of interference from fragments and side reactions (Dunne et al., 2012). Consequently, it remains uncertain whether the signal at m/z 42 was due to acetonitrile since the instrument cannot distinguish between isobaric compounds. However, we decided to present this mass in our results (section 3), as our measurements showed substantial amounts of it. In addition, the mass 63 is attributable to DMS. However, earlier studies



in the humid Amazon have found that acetaldehyde (mass 45) can form an agglomerate with water, resulting in the same mass (63). Thus, results for mass 63 attributed to DMS can be strongly influenced by acetaldehyde. We have studied the relation of the masses 63 and 45, and found a correlation coefficient of 0.51, indicating that a part of the observed 63 could indeed be acetaldehyde. Since we expect that a considerable part of the mass 63 is still originating from DMS, we focus our discussion of the mass 63 on the possible sources and sinks of DMS.

After PTR-QMS analysis, the bags were connected to a Los Gatos Ultraportable analyzer to measure the mixing ratios of CH<sub>4</sub> and CO<sub>2</sub>. The sample bag air was measured for 3 minutes with an airflow of ~ 0.1 LPM, and an average was taken from the last 2 minutes of the measurement.

## 2.6 BVOC & GHG flux calculation

To calculate BVOC and GHG fluxes, the Volumetric Mixing Ratios of the blank chamber bags (VMR<sub>b</sub>) were subtracted from the sample chamber bags (VMR):

$$dVMR = VMR - VMR_b \quad (1)$$

in which VMR is expressed in pptv or ppbv. By subtracting the mixing ratios of a blank chamber, dVMR represents the concentration difference attributable solely to soil and litter fluxes, corrected for potential chamber effects or the influence of ambient air entering the system. A dilution effect due to the constant sample flow is expected to exist but, at most, may lead to a slight underestimation of our fluxes. To convert dVMR to fluxes, we used:

$$F = dVMR * N * (V / A) * (1/T) \quad (2)$$

where N is the value of fixed molar volume at 25 °C (24.8 L mol<sup>-1</sup>; 40.3 mol m<sup>-3</sup>), V is the chamber volume (0.021 m<sup>3</sup>), A is the chamber area (0.0855 m<sup>2</sup>), and T is the average sampling time (25 min), giving fluxes in nmol m<sup>-2</sup> min<sup>-1</sup>, then converted to ng m<sup>-2</sup> h<sup>-1</sup>.

## 2.7 Soil and Litter Analyses

The Thematic Laboratory of Soils and Plants (LTSP, INPA) analyzed soil and litter nutrient content according to adapted protocols (EMBRAPA, 1999). The nutrients - iron (Fe<sup>+2</sup>), calcium (Ca<sup>+2</sup>), magnesium (Mg<sup>+2</sup>), zinc (Zn<sup>+2</sup>), potassium (K<sup>+</sup>), manganese (Mn<sup>+</sup>), phosphorus (P), and aluminum (Al) - were determined by digestion with a nitro-perchloric acid solution (Malavolta et al., 1989). Total phosphorus (P) was quantified using colorimetry (Murphy & Riley, 1962; Olsen



264 & Sommers, 1982) and measured using a UV spectrophotometer (Model 1240, Shimadzu, Kyoto,  
265 Japan). Potassium (K), calcium (Ca), and magnesium (Mg) concentrations were determined by  
266 atomic absorption spectrophotometry (AAS, 1100 B, 250 Perkin Elmer, Ueberlingen, Germany),  
267 as described by Anderson and Ingram (1993). Soil carbon and nitrogen content was determined by  
268 the Routine Measurements & Analyses Lab (RoMA, MPI-BGC) with the elemental analyzer  
269 "varioEL" (Elementar Analysensysteme GmbH, Elementar-Straße 1, D-63505 Langenselbold,  
270 Germany). Soil porosity was analyzed using the pycnometer method described in Flint & Flint  
271 (2002). The amount of water was corrected for soil density.

272 For analysis of soil and litter microbial Carbon, Nitrogen, and Phosphorus (C, N, and P) contents,  
273 2g of fresh litter and 5g of fresh soil were used from each sample chamber. These were separated  
274 into fumigated and non-fumigated samples. The fumigated samples were left with chloroform for  
275 24 hours and then divided into two sub-samples. For first, 50 mL of KCl (Potassium Chloride) was  
276 added, and total C and N were extracted, and for the second, 50 mL of NaHCO<sub>3</sub> (Sodium  
277 Bicarbonate) was added for total P extraction. Following the same extraction protocol, the non-  
278 fumigated samples were prepared for direct extraction without going through the 24-hour  
279 fumigation period. Microbial C, N, and P content was estimated in fumigated and non-fumigated  
280 extracts from the difference in organic C, N, and total P measured by a TOC/TN analyzer  
281 (Jenkinson et al., 2004). The extraction of the microbial biomass was performed at INPA, and the  
282 analyses were done by the Routine Measurements & Analyses Lab (RoMA, MPI-BGC).

## 283 **2.8 Statistical analyses**

284 A total of 36 samples were evaluated ( $n = 12$  per forest type). Gas fluxes were first correlated with  
285 potential predictors (soil and litter characteristics, Table 2), revealing variations between forest  
286 types. Separate regression models were built for each forest type to maximize predictive ability,  
287 with variable selection based on the following criteria: 1) given the statistical power limitation of  
288 models ( $n = 12$ ), the maximum number of independent variables possible to include was two; thus,  
289 2) we tested all models with one or two independent variable combinations; 3) finally, we chose  
290 the models which showed no multicollinearity and had the highest adjusted R-squared and lowest  
291 Akaike's information criterion (AIC). The "ols\_step\_all\_possible" function from the "olsrr"  
292 package (Hebbali, 2024) was used, and multicollinearity was assessed via VIF ( $<2.5$ ; Hair et al.,  
293 2009). Principal Component Analysis (PCA) and Pearson's correlation (Hmisc package; Harrell,



2018) were performed to explore variable interactions. Variations within forest types (e.g., between transects) were analyzed using t-tests for normal data and Kruskal-Wallis tests for non-normal data, with a significance level of 0.05. All analyses were conducted in R (v4.3.0; R Core Team, 2023).

298

299 **Table 2.** Variables, their respective codes, and units.

| Variable                          | Code          | Unit                   |
|-----------------------------------|---------------|------------------------|
| Soil carbon                       | c_soil        | %                      |
| Soil nitrogen                     | n_soil        | %                      |
| Soil phosphorus                   | p_soil        | P mg/kg                |
| Soil potassium                    | k_soil        | K <sup>+</sup> mg/kg   |
| Soil calcium                      | ca_soil       | Ca <sup>+2</sup> mg/kg |
| Soil magnesium                    | mg_soil       | Mg <sup>+2</sup> mg/kg |
| Soil aluminum                     | al_soil       | Al <sup>+3</sup> mg/kg |
| Soil iron                         | fe_soil       | Fe <sup>+2</sup> mg/kg |
| Soil zinc                         | zn_soil       | Zn <sup>+2</sup> mg/kg |
| Soil manganese                    | mn_soil       | Mn <sup>+2</sup> mg/kg |
| Soil ph                           | ph_soil       | pH                     |
| Soil temperature                  | soil_temp     | Celsius                |
| Soil moisture                     | soil_moisture | %                      |
| Litter carbon                     | c_litter      | %                      |
| Litter nitrogen                   | n_litter      | %                      |
| Litter calcium                    | ca_litter     | Ca <sup>+2</sup> mg/kg |
| Litter magnesium                  | mg_litter     | Mg <sup>+2</sup> mg/kg |
| Litter potassium                  | k_litter      | K <sup>+</sup> mg/kg   |
| Litter iron                       | fe_litter     | Fe <sup>+2</sup> mg/kg |
| Litter zinc                       | zn_litter     | Zn <sup>+2</sup> mg/kg |
| Litter manganese                  | mn_litter     | Mn <sup>+2</sup> mg/kg |
| Microbial biomass soil carbon     | c_mic_soil    | g/kg                   |
| Microbial biomass soil nitrogen   | n_mic_soil    | g/kg                   |
| Microbial biomass soil phosphorus | p_mic_soil    | g/kg                   |
| Microbial biomass litter carbon   | c_mic_litter  | g/kg                   |
| Microbial biomass litter nitrogen | n_mic_litter  | g/kg                   |
| Microbial biomass soil phosphorus | p_mic_litter  | g/kg                   |

300

301

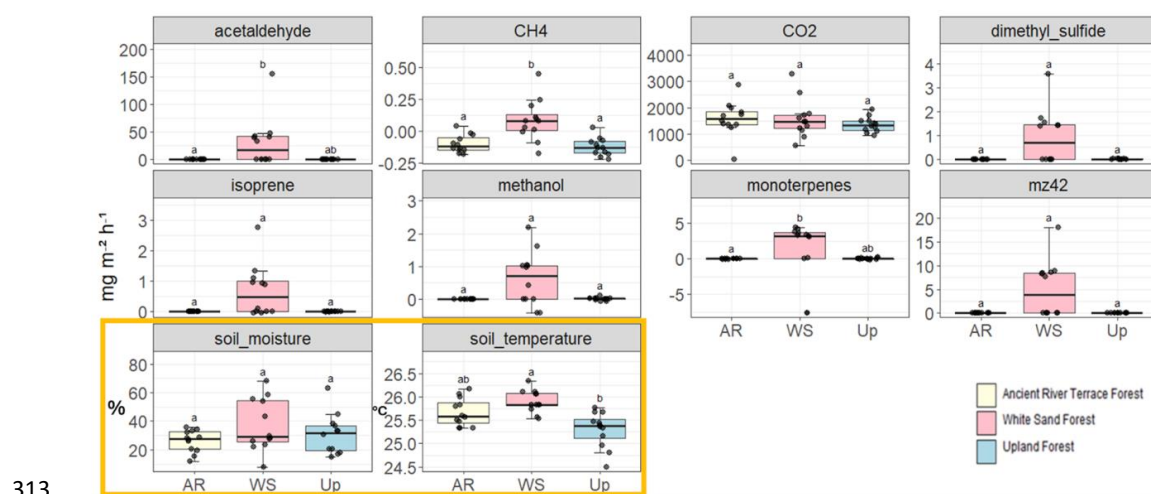


302

### 303 3. Results

#### 304 3.1 Comparison between forest types

305 The three forest types showed very different gas fluxes for BVOCs and GHGs (Fig. 3),  
306 with the highest fluxes observed in the white sand forest. Fluxes were very low in the upland forest,  
307 and almost no gas fluxes were observed in the ancient river terrace forest. Acetaldehyde emissions  
308 showed the most significant differences between forest types, with emission averages of 29.911  
309  $\text{mg m}^{-2} \text{h}^{-1}$  and 0.0885  $\text{mg m}^{-2} \text{h}^{-1}$  for white sand forest and upland forest, respectively, and low  
310 consumption for the ancient river terrace forest (-0.0140  $\text{mg m}^{-2} \text{h}^{-1}$ ). Isoprenoid (isoprene and  
311 monoterpenes) emissions were also high in the white sand forest, and clear differences were found  
312 between forest types concerning the speciation of monoterpenes (supplementary material; Fig. S2).



313

314 **Figure 3.** BVOC and GHG fluxes from soil and litter across the three forest types: ancient river  
315 terrace forest (AR), white sand forest (WS), and upland forest (Up). Letters indicate statistically  
316 significant differences in fluxes between forest types at  $p < 0.05$ ,  $N=36$  (Kruskal-Wallis test for  
317 non-normal data - BVOC and GHG). The yellow rectangle represents soil moisture (soil moisture  
318 expressed as % and soil temperature expressed as  $^{\circ}\text{C}$ ), and soil temperature (ANOVA test for  
319 normal distribution). Boxes show median and first and third quartiles, with whiskers and points  
320 distinguished at 1.5 times the interquartile range.



321 In the white sand forest, in addition to the high isoprenoid emissions, we also observed the  
322 consumption of monoterpenes ( $-7.628 \text{ mg m}^{-2} \text{ h}^{-1}$ , outlier in Fig. 3) and high emission of dimethyl  
323 sulfide (DMS) ( $0.924 \text{ mg m}^{-2} \text{ h}^{-1}$ , on average). Upland and ancient river terrace forests exhibited a  
324 small amount of DMS consumption.  $\text{CH}_4$  fluxes substantially varied in the white sand forest, with  
325 large uptake and emission fluxes, while ancient river terrace and upland forests both showed  
326 mainly  $\text{CH}_4$  uptake. There were no statistically significant differences in soil moisture between the  
327 forest types (Fig. 3); however, the white sand forest showed the highest and the lowest soil  
328 moisture values. Differences in soil moisture and temperature were found between transects (Fig.  
329 8). The large difference in soil texture (see supplementary material, table S1) between the sites  
330 will affect how soil moisture translates to the amount of soil moisture available for plants and  
331 microbes. Still, since individual transects were measured on different (consecutive) days, it is  
332 difficult to distinguish temporal from spatial effects.



334 **Figure 4.** Concentrations of soil micro- and macronutrients in the three forest types: ancient river  
335 terrace forest (AR), white sand forest (WS), and upland forest (Up). Letters indicate statistically





significant differences in nutrients between forest types at  $p < 0.05$ ,  $N=36$ . (ANOVA test for normal data (aluminum) and Kruskal-Wallis test for non-normal data (carbon, calcium, iron, potassium, magnesium, manganese, nitrogen, phosphorus, pH, and zinc). Boxes show median and first and third quartiles, with whiskers and points distinguished at 1.5 times the interquartile range.

Soil macro- and micronutrients varied considerably between the forest types, with statistically significant differences in carbon, magnesium, phosphorus, and iron for the white sand forest. Phosphorus content was the highest in the white sand forest compared to other forest types (Fig. 4). All litter nutrients exhibited significant differences between forest types: upland forest showed the highest average concentrations of calcium, iron, manganese, and zinc, while the ancient river terrace forest had the highest nitrogen, potassium, and phosphorus concentrations, and the white sand forest had slightly higher carbon concentrations (Fig. 5).

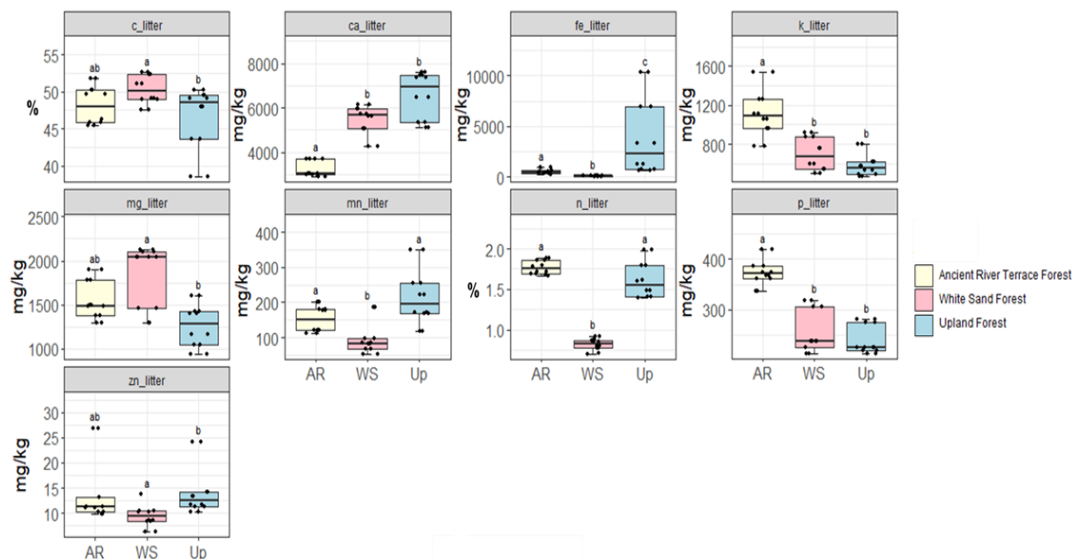


**Figure 5.** Concentrations of litter micro- and macronutrients in the three forest types: ancient river terrace forest (AR), white sand forest (WS), and upland forest (Up). Letters indicate statistically significant differences in nutrients between forest types at  $p < 0.05$ ,  $N=36$ . (ANOVA test for normal data - potassium and nitrogen, and Kruskal-Wallis test for non-normal data - carbon,



calcium, iron, magnesium, manganese, phosphorus, and zinc). Boxes show median and first and third quartiles, with whiskers and points distinguished at 1.5 times the interquartile range.

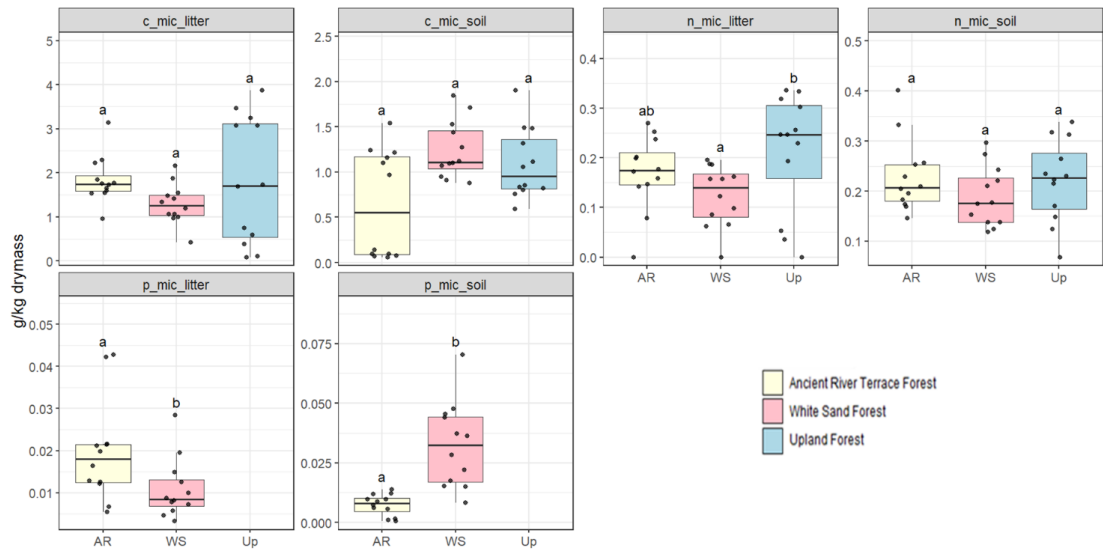


**Figure 6.** Concentrations of C, N, and P microbial biomass ( $\mu\text{g g}^{-1}$  dry mass) of soil and litter in the three forest types: the ancient river terrace forest (AR), the white sand forest (WS), and the upland forest (Up). Letters indicate statistically significant differences in microbial biomass between forest types at  $p < 0.05$ ,  $N=36$ . ANOVA test for normal data (litter microbial carbon, soil microbial phosphorus, and nitrogen) and Kruskal-Wallis test for non-normal data (soil microbial carbon, litter microbial nitrogen, and litter microbial phosphorus). Boxes show median and first and third quartiles, with whiskers and points distinguished at 1.5 times the interquartile range.

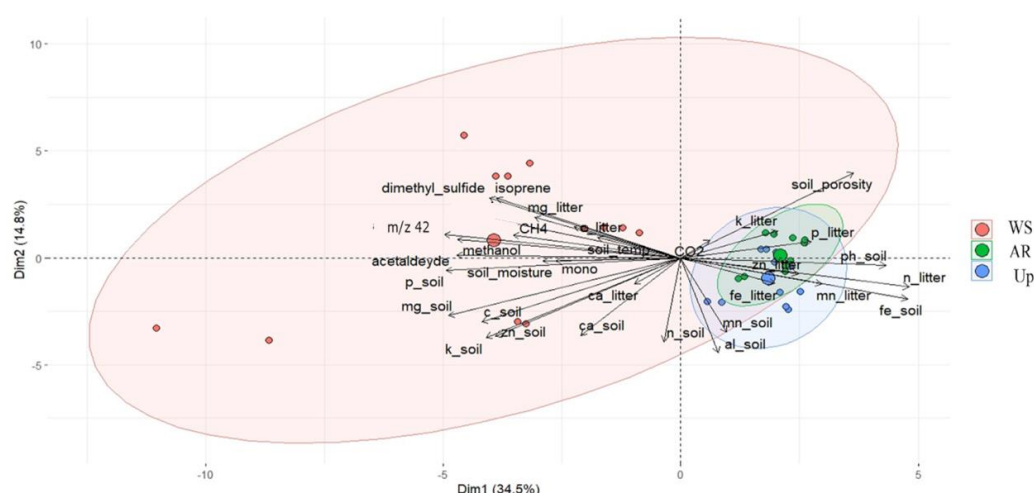
Microbial biomass (soil and litter) - measured as a potential proxy for microbial activity - showed significant differences between forest types. Soil microbial phosphorus was significantly higher in the white sand forest than in the ancient river terrace forest (no data for the upland forest). In contrast, litter microbial biomass (carbon and nitrogen) was the highest in the upland forest and the lowest in the white sand forest (carbon, nitrogen, phosphorus) (Fig. 6).

### 3.2 Identification of drivers of BVOC and GHG fluxes

#### 3.2.1 Principal Component Analysis



369 A Principal Component Analysis (PCA) of soil and litter characteristics and microbial  
370 biomass, and gas fluxes (BVOC and GHG) indicated that PC1 and PC2 axes accounted for 48.5%  
371 of the data variation (Fig. 7). The first axis explained 31.6% and the second 12.6% (Table 3). The  
372 PCA grouped forest types into two distinct groups: ancient river terrace and upland forests showed  
373 considerable overlap, with lower fluxes linked to litter characteristics, soil and litter microbial  
374 biomass, CO<sub>2</sub>, and soil pH; in contrast, the white sand forest formed a separate group with higher  
375 fluxes associated with soil temperature, moisture, and elevated levels of phosphorus, magnesium,  
376 and potassium.



377

378 **Figure 7.** Principal Component Analysis (PCA), wherein the vectors reflect their correlation with  
379 the variables, and the colored circles represent the average PCA score related to each ambient. The  
380 analyzed variables are BVOCs (methanol, m/z 42, acetaldehyde, dimethyl sulfide, isoprene and  
381 monoterpenes), greenhouse gases (CH<sub>4</sub> and CO<sub>2</sub>), soil characteristics (carbon, nitrogen,  
382 phosphorus, potassium, calcium, magnesium, aluminum, iron, zinc, manganese, pH, temperature,  
383 and soil moisture), litter characteristics (carbon, nitrogen, calcium, magnesium, potassium, iron,  
384 zinc, manganese), and soil and litter microorganism dynamics (soil microbial nitrogen, soil  
385 microbial phosphorus, soil microbial carbon, litter microbial nitrogen, litter microbial phosphorus  
386 and litter microbial carbon).



**Table 3.** Percentage correlation values extracted from Principal Component Analysis (PCA; Fig. 7).

|                   | PC1     |                  | PC2     |
|-------------------|---------|------------------|---------|
| Soil iron         | 83.480  | Isoprene         | 52.345  |
| Litter nitrogen   | 83.440  | Dimethyl sulfide | 51.718  |
| Litter manganese  | 52.649  | Litter Iron      | 21.662  |
| Litter phosphorus | 46.040  | Soil moisture    | 20.658  |
| Soil magnesium    | -79.524 | Soil carbon      | -63.818 |
| Methanol          | -80.097 | Soil zinc        | -64.436 |
| Soil phosphorus   | -83.184 | Soil aluminum    | -71.054 |
| m/z 42            | -84.917 | Soil nitrogen    | -71.553 |

### 3.2.2 Linear regression models for different forest types

We used linear regression models (referred to as linear models) to better understand the relationships between predictor variables and fluxes, as identified by the PCA analyses. Flux predictors showed substantial variation between the forest types (Fig. S3a, b, S4a, b, and S5a, b, in supplementary material). Model comparisons for each forest type revealed similarities between ancient river terrace (Table 4) and upland forests (Table 5). In contrast, the white sand forest (Table 6) was distinct, as also shown by the PCA analysis. In the ancient river terrace forest, linear models for gas fluxes and predictor variables showed coefficients of determination ( $R^2$ ) above 0.8 for methanol, acetaldehyde, isoprene, and monoterpenes (Table 4). The most important nutrients for predicting gas fluxes from the ancient river terrace forest were potassium, manganese, magnesium, iron, carbon, and phosphorus. The linear models for monoterpenes had the soil microbial biomass carbon and litter potassium as predictors. The GHG models had soil temperature, soil moisture, and litter nutrients as predictors.

**Table 4.** Multiple linear regression models with soil and litter characteristics and microbial biomass as predictors of gas fluxes in the ancient river terrace forest. B = unstandardized coefficients. CI = confidence interval.  $f^2$  = Cohen's  $f^2$  effect size.  $R^2$  = R-squared value.  $R^2_{adj}$  = Adjusted R-squared value. N = 12.



| Variable                | B       | 95% CI            | P      | f <sup>2</sup> | R <sup>2</sup> | R <sup>2</sup> <sub>adj</sub> |
|-------------------------|---------|-------------------|--------|----------------|----------------|-------------------------------|
| <b>Methanol</b>         |         |                   |        |                | 0.839          | 0.803                         |
| Soil potassium          | 0.034   | 0.021; 0.047      | < .001 | 2.222          |                |                               |
| Litter manganese        | 0.000   | 0.000; 0.000      | < .001 | 2.972          |                |                               |
| <b>Acetaldehyde</b>     |         |                   |        |                | 0.829          | 0.791                         |
| Soil iron               | 0.000   | -0.001; 0.000     | < .001 | 0.127          |                |                               |
| Soil manganese          | 0.004   | 0.003; 0.005      | < .001 | 4.711          |                |                               |
| <b>Dimethyl sulfide</b> |         |                   |        |                | 0.635          | 0.554                         |
| Soil magnesium          | 0.006   | 0.001; 0.010      | 0.016  | 0.059          |                |                               |
| Litter magnesium        | -0.004  | -0.006; -0.002    | 0.004  | 1.679          |                |                               |
| <b>Isoprene</b>         |         |                   |        |                | 0.969          | 0.963                         |
| Soil Iron               | 0.000   | 0.000; 0.000      | < .001 | 4.452          |                |                               |
| Soil Manganese          | 0.001   | 0.000; 0.001      | < .001 | 27.279         |                |                               |
| <b>Monoterpenes</b>     |         |                   |        |                | 0.920          | 0.902                         |
| Soil microbial carbon   | 0.000   | 0.000; 0.000      | < .001 | 10.81          |                |                               |
| Litter potassium        | 0.03    | 0.000; 0.05       | 0.026  | 0.78           |                |                               |
| <b>CH<sub>4</sub></b>   |         |                   |        |                | 0.276          | 0.203                         |
| Soil moisture           | 0.00    | 0.00; 0.00        | 0.0824 | 0.50           | 0.452          | 0.330                         |
| Litter carbon           | 0.00    | 0.00; 0.00        | 0.024  | 0.32           |                |                               |
| <b>CO<sub>2</sub></b>   |         |                   |        |                | 0.685          | 0.615                         |
| Soil temperature        | 9.054   | 3.101; 15.007     | 0.007  | 1.232          |                |                               |
| Litter phosphorus       | -87.940 | -156.215; -19.666 | 0.017  | 0.943          |                |                               |

408

409 For the upland forest, gas flux models showed R<sup>2</sup> higher than 0.8 for isoprene and CH<sub>4</sub>  
410 (Table 5). Key nutrients for predicting gas fluxes included potassium, iron, manganese, and  
411 carbon. Microbial biomass was significant in predicting gases like methanol and dimethyl sulfide.  
412 Acetaldehyde and isoprene shared soil iron and manganese as predictors, while dimethyl sulfide  
413 and CO<sub>2</sub> were linked to litter carbon and microbial nitrogen.

414 **Table 5.** Multiple linear regression models with soil and litter characteristics as predictors of gas  
415 fluxes in the upland forest. B = unstandardized coefficients. CI = confidence interval. f<sup>2</sup> = Cohen's  
416 f<sup>2</sup> effect size. R<sup>2</sup> = R-squared value. R<sup>2</sup><sub>adj</sub> = Adjusted R-squared value. N = 12.



| Variable                  | B     | 95% CI       | p      | f <sup>2</sup> | R <sup>2</sup> | R <sup>2</sup> <sub>adj</sub> |
|---------------------------|-------|--------------|--------|----------------|----------------|-------------------------------|
| <b>Methanol</b>           |       |              |        |                | 0.735          | 0.676                         |
| Soil potassium            | 0.77  | 0.41; 1.1    | 0.001  | 0.82           |                |                               |
| Soil microbial nitrogen   | 0.00  | 0.00; 0.00   | 0.002  | 1.96           |                |                               |
| <b>m/z 42</b>             |       |              |        |                | 0.679          | 0.608                         |
| Soil potassium            | 0.000 | 0.000; 0.001 | 0.002  | 0.687          |                |                               |
| Soil microbial nitrogen   | 0.000 | 0.000; 0.000 | 0.006  | 1.417          |                |                               |
| <b>Acetaldehyde</b>       |       |              |        |                | 0.793          | 0.748                         |
| Soil iron                 | 0.00  | 0.00; 0.00   | < .001 | 0.05           |                |                               |
| Soil manganese            | 0.02  | 0.1; 0.02    | 0.02   | 3.80           |                |                               |
| <b>Dimethyl sulfide</b>   |       |              |        |                | 0.775          | 0.725                         |
| Litter microbial carbon   | 0.00  | 0.00; 0.00   | <0.001 | 1.44           |                |                               |
| Litter microbial nitrogen | 0.00  | 0.00; 0.00   | 0.002  | 2.01           |                |                               |
| <b>Isoprene</b>           |       |              |        |                | 0.899          | 0.877                         |
| Soil iron                 | 0.00  | 0.00; 0.00   | < .001 | 5.48e-03       |                |                               |
| Soil manganese            | 0.00  | 0.00; 0.00   | < .001 | 5.94           |                |                               |
| <b>Monoterpenes</b>       |       |              |        |                | 0.695          | 0.627                         |
| Soil potassium            | 1.18  | 1.3;2.3      | < .001 | 2.94           |                |                               |
| Litter microbial nitrogen | 0.00  | 0.00;0.00    | < .001 | 4.63           |                |                               |
| <b>CH<sub>4</sub></b>     |       |              |        |                | 0.888          | 0.863                         |
| Soil carbon               | 0.231 | 0.00; 0.00   | 0.043  | 0.06           |                |                               |
| Soil moisture             | 0.00  | 0.00; 0.00   | < .001 | 7.91           |                |                               |
| <b>CO<sub>2</sub></b>     |       |              |        |                | 0.626          | 0.543                         |
| Litter microbial nitrogen | 0.00  | 0.01; 0.06   | 0.025  | 0.25           |                |                               |
| Litter microbial carbon   | 0.00  | 0.00;0.00    | 0.006  | 1.43           |                |                               |

417

418 In the white sand forest, models for methanol, m/z 42 and monoterpenes showed high R<sup>2</sup>  
419 values, explaining over 80% of emission variation (table 6). Key nutrient predictors included  
420 phosphorus, nitrogen, and zinc. All emitted gases (except CO<sub>2</sub>) were influenced by soil  
421 temperature or moisture. Soil temperature was inversely related to fluxes of methanol, DMS, and  
422 isoprene, while emissions of m/z 42, acetaldehyde, monoterpenes and CH<sub>4</sub> increased with soil  
423 moisture.





**Table 6.** Multiple linear regression models with soil and litter characteristics as predictors of gas fluxes in the white sand forest. B = unstandardized coefficients. CI = confidence interval.  $f^2$  = Cohen's  $f^2$  effect size.  $R^2$  = R-squared value.  $R^2_{adj}$  = Adjusted R-squared value. N = 12.

| Variable                | B        | 95% CI            | p       | $f^2$ | $R^2$ | $R^2_{adj}$ |
|-------------------------|----------|-------------------|---------|-------|-------|-------------|
| <b>Methanol</b>         |          |                   |         |       | 0.825 | 0.790       |
| Soil temperature        | -0.064   | -3.4, -0.46       | < 0.015 | 4.21  |       |             |
| Litter phosphorus       | -8.4     | -16,-0.37         | < 0.042 | 0.62  |       |             |
| <b>Acetonitrile</b>     |          |                   |         |       | 0.866 | 0.837       |
| Soil moisture           | 0.187    | 0.099; 0.276      | < .001  | 2.938 |       |             |
| Litter nitrogen         | -54.196  | -75.901; -32.491  | < .001  | 3.545 |       |             |
| <b>Acetaldehyde</b>     |          |                   |         |       | 0.653 | 0.576       |
| Soil moisture           | 1.368    | 0.284; 2.452      | 0.019   | 1.022 |       |             |
| Litter nitrogen         | -327.465 | -593.333; -61.596 | 0.021   | 0.863 |       |             |
| <b>Dimethyl sulfide</b> |          |                   |         |       | 0.784 | 0.736       |
| Soil temperature        | -0.32    | -4.9; -1.4        | 0.003   | 1.87  |       |             |
| Soil phosphorus         | -0.06    | -0.09,-0.03       | 0.003   | 1.36  |       |             |
| <b>Isoprene</b>         |          |                   |         |       | 0.764 | 0.712       |
| Soil temperature        | -1.988   | -3.6; -0.96       | 0.003   | 1.70  |       |             |
| Soil phosphorus         | -0.05    | -0.007; -0.02     | 0.004   | 1.54  |       |             |
| <b>Monoterpene</b>      |          |                   |         |       | 0.857 | 0.825       |
| Soil moisture           | 0.13     | 0.06; 0.20        | 0.003   | 0.36  |       |             |
| Litter nitrogen         | 2.1      | 1.5; 2.8          | < 0.001 | 5.66  |       |             |
| <b>Sesquiterpene</b>    |          |                   |         |       | 0.888 | 0.863       |
| Soil moisture           | 1.1      | 0.52;1.7          | 0.002   | 2.50  |       |             |
| Litter nitrogen         | -435     | -5.75; -294       | < 0.001 | 5.43  |       |             |
| <b>CH<sub>4</sub></b>   |          |                   |         |       | 0.508 | 0.399       |
| Soil moisture           | 0.0      | 0.0; 0.0          | 0.027   | 0.35  |       |             |
| Litter zinc             | 0.0      | 0.0; 0.0          | 0.035   | 0.69  |       |             |
| <b>CO<sub>2</sub></b>   |          |                   |         |       | 0.742 | 0.685       |
| Soil microbial carbon   | 0.02     | 0.0; 0.03         | 0.029   | 1.07  |       |             |
| Litter zinc             | 3.5      | 1.6; 5.5          | 0.003   | 1.81  |       |             |



3.3 Spatial variability within forest types

Figure 8 shows BVOC and GHG fluxes of each transect, and Figure 9 illustrates the spatial variability within and between transects of isoprene and monoterpenes (see supplementary material, Fig. S8, S9, and S10 for other gases). In the ancient river terrace forest, BVOC fluxes were generally lower in transect 1, while GHG fluxes were similar between transects (Fig. 8). The soil temperature was higher in transect 1, while transect 2 was slightly wetter (although not statistically significant). The white sand forest exhibited the greatest variation between transects, with the highest BVOC emissions in transect 2, and significant variations in acetaldehyde, m/z 42, dimethyl sulfide, isoprene, and methanol. In addition, monoterpene fluxes showed high variation in emissions and consumption in transect 1, while transect 2 had low variation and high emissions. Furthermore, methanol was emitted in transect 1 and consumed in transect 2. In the upland forest, significant differences between transects were noted for acetaldehyde, m/z 42, dimethyl sulfide, and isoprene. For the ancient river terrace forest, the gas fluxes between transects were similar with only few variations in GHG fluxes, however significant differences in isoprene fluxes were observed.

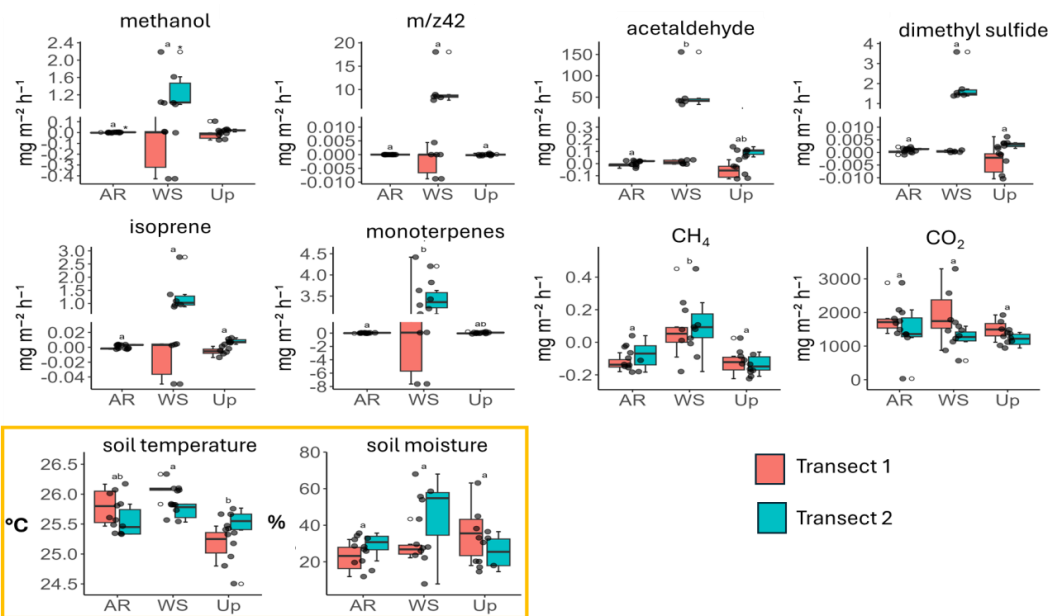
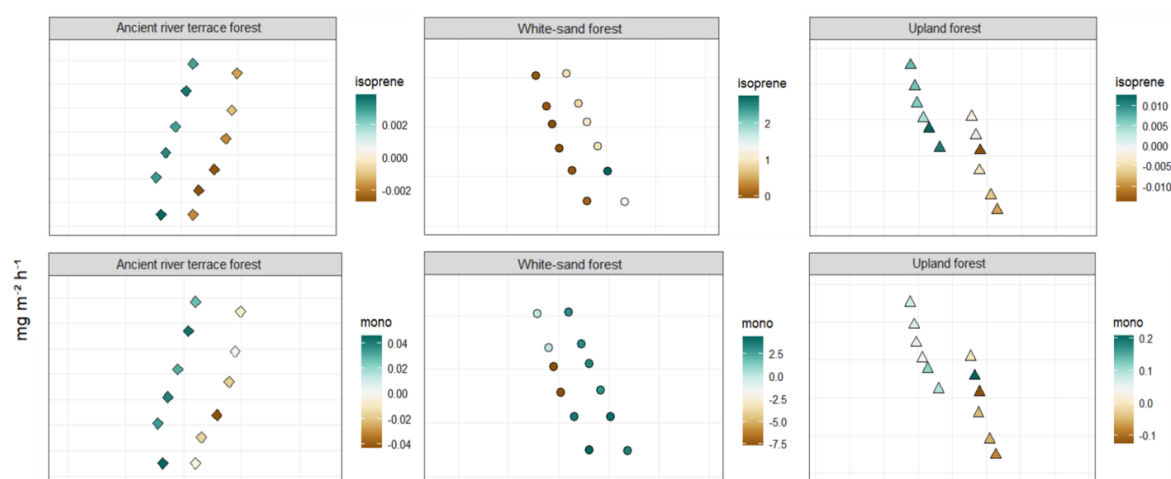




**Figure 8.** Soil and litter BVOC and GHG fluxes in each forest type - ancient river terrace forest (AR), white sand forest (WS), upland forest (Up), and transects within. Letters indicate statistically significant differences in fluxes between the forest types at  $p < 0.05$ ,  $N=36$  (Kruskal-Wallis test for non-normal data - BVOC and GHG). The yellow rectangle represents soil moisture and temperature plots (ANOVA test for normal distribution). Boxes show median and first and third quartiles, with whiskers and points distinguished at 1.5 times the interquartile range. Axes are broken to enhance the visibility of data variation.

452



453

**Figure 9.** Map of the sampling points visualizing the spatial heterogeneity of BVOC fluxes in each of the three forest types. Each transect, sampled on different but subsequent days, contains six sampling points, totaling 12 measurement points per forest type. Left - Transect 1; Right - transect 2. Mono = Monoterpenes. The gas flux data are expressed in  $\text{mg m}^{-2} \text{h}^{-1}$ .

#### 4. Discussion

Previous studies investigated tropical soil BVOC fluxes with incubation (Bourtsoukidis et al., 2018) and fertilization experiments (Llusià et al., 2022). These studies gave insights into how BVOC soil fluxes respond to drought and nutrients, and suggested their magnitudes are much higher than anticipated. The present study found that soil-litter BVOC and GHG fluxes changed across Amazonian forest types and were influenced by differences in nutrient content, soil



moisture and temperature, and microbial biomass. The main differences in soil-litter properties, soil-litter gas fluxes, their interaction with soil-litter properties across forest types, and the significance of our findings are discussed in the following sections.

Given the extensive number of measured variables, we chose to focus our discussion on the most relevant and novel findings related to BVOC and CH<sub>4</sub> fluxes and their drivers, rather than covering all variables and fluxes. However, since these variables may still be of interest to the reader, detailed analyses are provided in the supplementary material.

#### **4.1 Differences in soil and litter nutrient contents across forest types**

Soil and litter properties showed strong differences between forest types. The ancient river terrace forest stood out for its high litter K and P contents, though the underlying mechanisms—such as nutrient resorption efficiency or soil nutrient availability—remain to be investigated. In the upland forest, the dominance of soil iron is likely related to the intense leaching common in oxisols, resulting in iron enrichment due to the removal of other nutrients (Mosquera et al., 2024); in addition, the formation of iron oxides reduces the mineralization of organic matter, promoting iron accumulation in the leaf litter (Li et al., 2023).

Overall, the white sand forest exhibited distinct soil properties compared to the other studied forest types. Despite its well-documented low fertility (Mendonça et al., 2015; Demarchi et al., 2022), this forest type showed unexpectedly high soil nutrient and carbon concentrations. Phosphorus levels were up to four times higher than in upland and ancient river terrace forests, potentially due to dissolved organic nutrients mitigating nutrient limitations (Lange et al., 2024). While earlier studies reported higher carbon content in upland forests (Marques et al., 2017), the white sand forest's extensive root mats may enhance carbon storage, as observed in structurally analogous ecosystems (Draper et al., 2014). Iron concentrations in the soil of white sand forest were lower than expected (Cornu et al., 1997), possibly due to spatial variability and seasonal dynamics. During the dry season, low water retention in sandy soils induces drought stress, while wet-season leaching redistributes iron, aluminum, and magnesium (García-Villacorta et al., 2016). This process can form cemented horizons, impeding drainage and elevating water tables (Franco & Dezzio, 1994; Demarchi et al., 2022). Additionally, differences in tree species composition



492 between forest types may influence nutrient levels (García-Villacorta et al., 2016; Gomes Alves et  
493 al., 2022).

#### 494 **4.2 Differences in gas fluxes across the different forest types**

495 Our results revealed that the white sand forest showed the highest emissions and consumption of  
496 gases, accompanied by the greatest chemical diversity in fluxes. This elevated chemical diversity  
497 may be attributed to the distinct characteristics of the white sand forest, such as its unique  
498 microbiome, seasonality, and species composition (Rinnan et al., 2013; Viros et al., 2021;  
499 Vermeuel et al., 2023). Species endemic to this ecosystem may influence BVOC emission patterns  
500 and speciation. Fine et al. (2004, 2006) showed that tree species adapted to very nutrient-poor  
501 sandy soils highly invest in secondary metabolite compounds in defense against herbivory, since  
502 leaves are very energetically costly for the plant. This large quantity of secondary compounds can  
503 directly influence litter decomposition rate (Chomel et al., 2016) and probably release gases and  
504 various compounds into the soil and water (Caetano, 2022).

505 Isoprenoids were emitted in considerable amounts in the white sand forest. As isoprenoids are not  
506 expected to be emitted from soil (Bach & Rohmer, 2013; Asensio et al., 2008), the observed high  
507 emissions could be attributed to the activity of microorganisms living in the soil and litter  
508 (Carruthers & Lee, 2021; Hernandez-Arranz et al., 2019). In addition, it is important to note that,  
509 although emissions in this study are expected to come from soil and litter, the contribution of root  
510 emissions cannot be ruled out, as the main source of isoprenoids is expected to be the plant  
511 metabolism (Pulido et al., 2012; Thulasiram et al., 2007).

512 A previous study on experimental rainforest soils - similar to upland forest soils - showed BVOC  
513 soil uptake (under wet conditions) primarily for isoprenoids, carbonyls, and alcohols, as well as  
514 soil emissions of dimethyl sulfide and carbonyl compounds such as acetaldehyde and acetone  
515 (Pugliese et al., 2023). Our upland forest isoprene fluxes exhibited lower soil uptake ( $-0.1 \text{ mg m}^{-2}$   
516  $\text{h}^{-1}$ ) compared to the increased uptake fluxes under drier conditions ( $\sim -2.38 \text{ mg m}^{-2} \text{ h}^{-1}$ ) observed  
517 by Pugliese et al. (2023). In general, our upland and ancient river terrace forests showed lower  
518 average emissions and uptake than those reported by Pugliese et al. (2023). This could also be due  
519 to a greater observed abundance of atmospheric isoprene as described in Pugliese et al. (2023),  
520 leading to a larger uptake. A study focusing on methanol fluxes in cropland soils observed values



521 ranging from 0.53 to 2.93 mg m<sup>-2</sup> h<sup>-1</sup> (Liu et al., 2024), which are higher than those observed in  
522 the current study in upland and ancient river terrace forests but interestingly similar to the white  
523 sand forest fluxes (1.5 mg m<sup>-2</sup> h<sup>-1</sup>). These higher emissions in crop soils can likely be attributed to  
524 factors such as crop species, tillage, fertilization, and irrigation, which can all influence BVOC  
525 emission rates; whereas the high methanol emission observed in our study could be related to the  
526 root growth of white sand forest's extensive root mats (although future studies are necessary to  
527 confirm this hypothesis). Dimethyl sulfide emission fluxes were highest in the white sand forest  
528 (~ 0.92 mg m<sup>-2</sup> h<sup>-1</sup>), higher than the DMS emission of 5.76 µg m<sup>-2</sup> h<sup>-1</sup> reported by Jardine et al.  
529 (2015) for Amazon soils; however, it is important to note that the high magnitude of DMS fluxes  
530 presented here might be influenced by a potential agglomerate of acetaldehyde (mass 45) with  
531 water, resulting in the same mass as DMS (63), suggesting that future studies could make use of  
532 techniques that differentiate these compounds. A compound with a mass-to-charge ratio (m/z) of  
533 42 was observed in the white sand forest, but its identity could not be confirmed due to technical  
534 limitations (Dunne et al., 2012). This m/z 42 is frequently attributed to acetonitrile, a known  
535 biomass burning marker primarily associated with anthropogenic sources (Huangfu et al., 2021).  
536 However, since it can also be emitted by microorganisms (Raio et al., 2020), it is possible that the  
537 microbial communities of the white sand forest contributed to potential acetonitrile (m/z 42)  
538 emissions.

539 Methane uptake was observed in the upland (-0.12 mg m<sup>-2</sup> h<sup>-1</sup>) and ancient river terrace (-0.10 mg  
540 m<sup>-2</sup> h<sup>-1</sup>) forests, whereas emissions were observed in the white sand forest (0.12 mg m<sup>-2</sup> h<sup>-1</sup>). These  
541 results are probably explained by the shallow water table characteristic of this forest type, which  
542 makes the soil saturated and creates an anaerobic environment that favors the growth of methane-  
543 producing microorganisms (methanogens), contributing to the observed high emissions. In another  
544 central Amazonia site, upland forest methane fluxes of similar magnitude were observed (-0.02 to  
545 -0.09 mg m<sup>-2</sup> h<sup>-1</sup>) (van Asperen et al., 2020). However, white sand forest fluxes in their study  
546 showed uptake instead of emission (-0.38 to -0.25 mg m<sup>-2</sup> h<sup>-1</sup>). This difference is probably  
547 explained by the natural variations across white sand forest ecosystems, especially concerning  
548 water table depth (Franco & Dezzio, 1994; Demarchi et al., 2022).

#### 549 **4.3 General Drivers of Soil and Litter Fluxes**





550 A principal component analysis (PCA) was performed to identify variables that could collectively  
551 differentiate forest types and their gas fluxes. As the PCA showed a limited capacity for  
552 differentiation due to overlapping ellipses, a further investigation was carried out using linear  
553 models (LMs). The LMs showed that soil temperature and soil moisture were important physical  
554 drivers for all three forest types, especially for the white sand forest. Since the white sand forest  
555 presents a relatively open canopy, with shorter trees and a shallow water table (Adeney et al., 2016;  
556 Rossetti et al., 2019), it often experiences extreme conditions and short-term variation, as  
557 demonstrated by the highly variable temperature and soil moisture values measured over two  
558 transects, in two subsequent days. Here, we discuss the role of soil temperature and moisture, and  
559 other potential drivers of gas fluxes.

#### 560 **4.3.1 Soil moisture and soil temperature as drivers of soil and litter gas fluxes**

561 Soil temperature and moisture were significant drivers for most gases, especially in the white sand  
562 forest, which agrees with what has been observed in other ecosystems (Trowbridge et al., 2020;  
563 Pugliese et al., 2023; Liu et al., 2024). For example, Pugliese et al. (2023) observed that rainforest  
564 soils acted as net BVOC sinks under moist conditions and as net BVOC sources under dry  
565 conditions. By comparing two transects in the upland forest, we observed a similar pattern, with  
566 the wetter transect showing BVOC consumption while the drier transect showed emissions.  
567 However, in the white sand forest, high BVOC emissions were observed in the wetter transect,  
568 while low emissions and uptake were observed in the drier transect. This shows that Amazonian  
569 soil emissions may respond differently to soil moisture depending on the soil and forest type.  
570 Interestingly, soil moisture was shown to be a predictor for methane for all three forest types,  
571 suggesting a general mechanism influencing methane fluxes regardless of the forest type, and in  
572 agreement with several studies showing the relationship between methane flux and soil moisture  
573 (Bridgham et al., 2013; Conrad, 2009; Shah et al., 2024; Van Den Pol-van Dasselaar et al., 1998).

574 Generally, BVOC fluxes exhibited a positive correlation with soil moisture and an inverse  
575 relationship with soil temperature. However, since high soil moisture often coincides with low  
576 temperatures, it remains challenging to ascertain whether low temperatures or high moisture levels  
577 drive increased fluxes under field conditions. This complexity is particularly relevant given that  
578 BVOC uptake and emission are closely tied to biological processes, which typically correlate



579 positively with temperature. High temperatures can enhance BVOC emissions and, at the same  
580 time, stimulate biological uptake (Baggesen et al., 2022). Notably, biological uptake may respond  
581 more vigorously to elevated temperatures than biological BVOC emission, potentially resulting in  
582 lower net emissions or even uptake (Penuelas et al., 2014; Jiao et al., 2023). However, as this study  
583 was based on field measurements, wherein soil moisture and temperature are intertwined, it is not  
584 possible to disentangle their combined effects.

#### 585 **4.3.2 Forest type-specific drivers of soil and litter gas fluxes**

586 In general, ancient river terrace and upland forests showed many similarities in the predictors of  
587 certain gases. In contrast, other drivers were found in the white sand forest. Here we discuss the  
588 observed key drivers (soil potassium, carbon, phosphorus and microbial biomass) for each forest  
589 type.

590 For ancient river terrace and upland forests, soil potassium was a significant factor influencing soil  
591 fluxes, being identified as a predictor of methanol and monoterpenes. In addition, it was also  
592 identified as a predictor of m/z 42 fluxes in the upland forest. Although we have not found studies  
593 relating BVOC and GHG fluxes to soil potassium content, potassium is an essential macronutrient  
594 for plant growth and metabolism. Its availability can affect plant physiological processes (Wang  
595 et al., 2013) and microbial activity (Mazahar & Umar, 2022), which in turn can influence BVOC  
596 production and release. In the upland forest, methane consumption fluxes correlated well with soil  
597 carbon (in conjunction with soil moisture, as mentioned previously). Soil organic carbon is known  
598 to play an important role in supporting methanotrophic bacteria, which are responsible for methane  
599 oxidation (Lee et al., 2023); therefore, we suggest that the total soil carbon observed in our study  
600 might affect methane uptake through a similar process.

601 Phosphorus, like carbon, is a key nutrient in the soil and significantly affected BVOC fluxes,  
602 especially for methanol in the white sand forest. The relationship between phosphorus and BVOC  
603 emissions is well documented for plants since the availability of phosphorus can influence the  
604 production and emission of BVOCs (Ndah et al., 2022). However, some fertilization studies have  
605 also shown that increasing soil nutrient status (nitrogen, phosphorus, and potassium) can modify  
606 pH levels, affecting microorganisms and their health state (Stotzky et al., 1976) and directly or



607 indirectly promoting or inhibiting BVOC fluxes (Liu et al., 2024; Raza et al., 2017). Our findings  
608 in the white sand forest are consistent with this observation.

609 Interestingly, our results suggested that lower phosphorus levels were associated with higher  
610 isoprene emissions. The mechanisms behind this relationship remain unclear. However, Llusà et  
611 al., (2022) found that phosphorus fertilization is less efficient than nitrogen fertilization in  
612 increasing monoterpene and sesquiterpene emissions (they did not find isoprene emissions) in a  
613 tropical forest. They observed that emissions increased when the soil was fertilized only with  
614 nitrogen—consistent with a phosphorus-limited system—because excess nitrogen stimulates the  
615 enzymes responsible for producing monoterpenes and sesquiterpenes. Conversely, the addition of  
616 phosphorus likely redirected this nutrient toward plant growth, resulting in lower emissions of  
617 monoterpenes and sesquiterpenes in the phosphorus-fertilized plots compared to those fertilized  
618 with nitrogen. As in this study, there was no fertilization or a controlled environment, so we can  
619 not draw similar conclusions. However, our findings provide valuable insights into the possible  
620 interactions between phosphorus, nitrogen, and soil BVOC fluxes in tropical ecosystems. These  
621 observations align with previous studies on the influence of soil nutrients (Liu et al., 2024; Llusà  
622 et al., 2022) and we suggest future soil fertilization studies to explore these relationships across  
623 soil and forest types in Amazonia.

624 For the upland forest, it was found that microbial biomass was a significant driver for almost all  
625 gas fluxes, except for isoprene and methane. This aligns with previous studies that have identified  
626 microbial biomass as an important driver for soil gas fluxes (Leff & Fierer, 2008; Lamers et al.,  
627 2013; Mancuso et al., 2015; Carrion et al., 2017; Tang et al., 2019). For example, Lehnert et al.  
628 (2023) demonstrated that the degradation of organic matter is an important source of DMS  
629 emissions, highlighting the role of microorganisms associated with decomposition. Jardine et al.,  
630 (2015) point out that DMS emissions in Amazonian soils are related to microbial processes, which  
631 was also reported by Kesselmeier and Hubert (2002). DMS can be produced in anaerobic  
632 environments, such as saturated soils or lakes (Carrion et al., 2017; Lehnert et al., 2023). This may  
633 explain the high emissions observed in transect 2 (wetter and more saturated) of the white sand  
634 forest, where conditions favorable to anaerobic processes are common and frequently linked to the  
635 production of sulfur compounds such as DMS. In contrast, in the drier transect 1 of the upland  
636 forest, DMS consumption was observed, suggesting the occurrence of microbial uptake processes.



637 Previous studies, such as the one carried out by Eyice et al. (2015), have shown that bacteria can  
638 consume carbon from DMS as an energy source. Therefore, the observed uptake may be the result  
639 of microorganisms utilizing the carbon present in DMS as an energy source, leading to uptake  
640 rather than production. This dual role of microorganisms - as both producers and consumers of  
641 DMS - highlights the complexity of sulfur cycling in terrestrial ecosystems.

642 From the few studies investigating the relationship between microorganisms and BVOC dynamics,  
643 it has been shown that some Proteobacteria, Actinobacteria, and Firmicutes can produce isoprene  
644 (Kuzma et al., 1995; McGenity et al., 2018). *Bacillus subtilis* can produce isoprene in response to  
645 stress; however, the mechanism is still not clear (McGenity et al., 2018). Some studies have shown  
646 that reduced soil microbial diversity can increase BVOC fluxes and alter the chemical composition  
647 of emitted compounds (Abis et al., 2020; Saunier et al., 2020; Sillo et al., 2024). Although  
648 microbial community data were unavailable in this study, we suggest that potential differences in  
649 microbial diversity have influenced emission and consumption patterns. Therefore, we strongly  
650 recommend that future studies investigate gas flux measurements with microbial community  
651 analyses to better understand these dynamics.

#### 652 **4.4. Spatial and temporal variability effects on BVOC fluxes**

653 While efforts were made in this study to minimize the effects of spatial variability, such as by  
654 measuring equidistant points and selecting homogeneous areas, it is important to consider that  
655 spatial variability still inevitably influenced our results, as observed in other studies (Durán &  
656 Delgado-Baquerizo, 2020). With respect to temporal variability, the transects were measured at  
657 the same time (08:00–10:00 am, local time) but on consecutive days, so differences in gas fluxes,  
658 soil moisture, and temperature may partly reflect external factors like prior precipitation,  
659 cloudiness, and air temperature changes. Just before the measurement of transect 2 at the white  
660 sand forest, a heavy rainfall occurred. This coincides with the observation of significantly high  
661 BVOC emissions in this transect, while transect 1 showed much lower emissions and more uptake.  
662 Bourtsoukidis et al., (2018) also found that sesquiterpenes emissions from upland forest soils in  
663 the dry season (after a rain event) were comparable to those from vegetation, suggesting that soil  
664 moisture is a crucial factor influencing sesquiterpenes emissions from Amazonian soils. As we  
665 observed substantially high isoprene, monoterpenes and acetaldehyde emissions in transect 2 of



the white sand forest, we argue that these observed BVOC emissions represent a burst induced by the preceding rainfall event, similar to the observed increase in BVOC emissions during and immediately after rainfall in a *Ponderosa pine* plantation (Greenberg et al., 2012). Likewise, Jardine et al., (2016) observed a peak in DMS soil emissions after rainfall. Therefore, higher emissions are expected to result from the interlinked effects of soil temperature and moisture and, as described above, the possible physical effects of rainfall (Miyama et al., 2020).

#### 4.5 The relevance of white sand forest ecosystems

This study showed large variability across forest types and unexpectedly high BVOC emissions from the white sand forest. Relatively few studies have been performed on white sand forests, which can partly be explained by the challenging conditions of this forest type, such as flooding and extreme temperatures, which require specific infrastructure for data collection (Adeney et al., 2016). In addition, the complex nature of this ecosystem - characterized by scattered patches of differentiated vegetation distributed within extensive upland forests (Demarchi et al., 2022) - can make access to these sites even more difficult. It is acknowledged that BVOC and GHG studies in white sand forests are limited: so far, only one study has provided data on BVOC fluxes with soil incubation lab measurements (Bourtsoukidis et al., 2018), and another measuring GHGs in situ (van Asperen et al., 2020). Despite representing only 5% of the Amazon basin area (Adeney et al., 2016) and 8% of the Reserve of this study (Demarchi et al., 2022), white sand forests are extremely important environments. Their sandy, nutrient-poor soil type has created a challenging ecosystem for plant growth (Fine & Baraloto, 2016), and this unique condition has selected specialized flora and fauna adapted to thrive in these ecosystems (Adeney et al., 2016; Demarchi et al., 2022). This high level of endemism contributes significantly to the overall biodiversity of the Amazon Basin (García-Villacorta et al. 2016). Moreover, white sand forests have been shown to play a crucial role in the chemistry of dissolved organic matter (DOM) in Amazonian blackwater rivers, linking terrestrial ecosystem processes to aquatic biogeochemistry (Simon et al., 2021). Our results showed that white sand forest gas fluxes clearly depend on physical drivers (more than other forest types), which indicates a possible sensitivity to upcoming climate extremes. Although Costa et al. (2023) did not focus specifically on the white sand forest, they showed that regions of the Amazon with shallow water tables—such as the white sand forest—can act as hydrological refuges during droughts. In these areas, higher productivity under dry conditions may help offset the substantial



696 carbon losses typically observed in deep water table (upland) forests during drought. Therefore, it  
697 is crucial to recognize that white sand forests have historically been neglected, even with their  
698 critical role in regulating the carbon cycle and maintaining Amazonian biodiversity (Rossetti et  
699 al., 2019). As for BVOC and GHG measurements, even less information is available for this  
700 ecosystem. However, our results suggest that white sand forests may play a significant role in both  
701 the emission and uptake of these compounds, reinforcing their importance in regional carbon and  
702 trace gas fluxes. Notably, a recent study reported high atmospheric isoprene concentrations in the  
703 northwestern Amazon throughout most of the year (Wells et al., 2022) — a region characterized  
704 by extensive and continuous white sand forest cover (Borges et al., 2014). Together, these findings  
705 highlight the need to better integrate white sand forests into future flux studies and atmospheric  
706 models.

## 707 **5. Summary and future directions**

708 Multiple interconnected factors influence BVOC and GHG soil fluxes in the central Amazon. This  
709 study highlights the significant roles of soil and litter properties, as well as microbial biomass, in  
710 driving these fluxes, with distinct patterns observed across forest types. Given the complexity of  
711 the mechanisms influencing BVOC and GHG emissions, future studies should prioritize microbial  
712 activity and diversity, along with diurnal and seasonal cycles, to better identify the key drivers of  
713 emissions and consumption in these diverse forest ecosystems.

714 It is important to note that this research serves as a pilot study aimed at scoping out general trends,  
715 and many sampling issues can be addressed in future work. For instance, utilizing a PTR-ToF-MS  
716 could alleviate the challenges associated with measuring acetaldehyde, DMS and  $m/z$  42. Longer  
717 sampling periods, ideally continuous, would allow for capturing daily variations in emissions.  
718 Surprisingly, despite being the least fertile and diverse forest type, the white sand forest exhibited  
719 the highest uptake and emission fluxes. This is likely due to intrinsic environmental factors, such  
720 as soil temperature and moisture, influencing microbial activity and gas fluxes, as well as the  
721 unique vegetation composition of the white sand forest. Furthermore, external factors, like the  
722 preceding rainfall event, could have contributed to the observed high emissions. Therefore, future  
723 extending the measurement duration would provide a clearer understanding of how rainfall events  
724 influence average soil BVOC emissions. The exceptionally high emissions observed in the white





725 sand forest may reflect short-term bursts following rainfall, which could be moderated when  
726 averaging over longer periods that capture the full range of environmental conditions in these  
727 ecosystems. Still, white sand forests may serve as BVOC emission hotspots after rain events,  
728 potentially becoming even more significant under climate change. Despite their limited area, they  
729 could have substantial ecological and atmospheric impacts. We encourage further research into  
730 this ecosystem to better understand its ecological processes and role in atmospheric dynamics, as  
731 forest BVOC fluxes influence key physical and chemical processes in the atmosphere, ultimately  
732 affecting the climate system.

### 733 **Code/Data availability**

734 All data supporting the findings of this study will be made available in a public repository upon  
735 publication.

### 736 **Authors' contributions**

737 Débora Pinheiro Oliveira, Hella van Asperen, and Eliane Gomes Alves contributed to the  
738 development and design of the study, as well as the collection, processing, and statistical analysis  
739 of the datasets. Murielli Garcia Caetano and Michelle Robin contributed to field data collection  
740 and data analysis. Achim Edtbauer helped design the methodology used in the PTR-QMS and  
741 contributed to its calibration improvement. Nora Zannoni, Joseph Byron, Jonathan Williams,  
742 Sergio Duvoisin-Junior, and Carla Batista contributed to the chemical analysis of BVOC samples  
743 with the GC-TOF-MS and GC-MS. Layon Demarchi and Maria T. F. Piedade contributed to the  
744 data analysis of the white sand forest. Maria T. F. Piedade, Jochen Schöngart, and Florian  
745 Wittmann contributed to the dataset for the initial selection of the points in the PELD-MAUA  
746 project plots where the soil chambers were installed. Rodrigo Augusto Ferreira de Souza  
747 contributed to the development of the study. All authors contributed to the writing of the  
748 manuscript.

### 749 **Competing interests**

750 The authors declare that they have no conflict of interest.

### 751 **Acknowledgments**



We thank the National Institute for Amazonian Research (INPA) and the Max Planck Institute for Biogeochemistry (MPI-BGC) for their ongoing support. We would like to acknowledge the support of the ATTO project (German Federal Ministry of Education and Research, funds BMBF 01LB1001A, 01LK1602, 01LK2101; Brazilian Ministry of Science, Technology, Innovation and Communications; contract FINEP/MCTIC 01.11.01248.00); UEA and FAPEAM, LBA/INPA and SDS/CEUC/RDS-Uatumã. We would like to acknowledge the contribution of the DFG project 352322796, which enabled the use of the Ultraportable Greenhouse Gas Analyzer. We also truly thank the PELD-MAUA project (CNPq/MCTI/CONFAP-FAPs, grant number: 441811/2020-5 (CNPq); 01.02.016301.02630/2022-76 (FAPEAM)) for the plots used in this study. We would also like to thank the field assistants, Jose Raimundo Ferreira Nunes and Sipko Bulthuis; and all the people involved in the logistical support of the ATTO project (André Almeida, Delano Campos, Amaury Rodrigues, Nagib Alberto, Valmir and Antonio Huxley), especially Roberta de Souza, who were essential to the development of this study. We also thank the technicians and assistants at INPA's soil laboratories - LTSP and Routine Measurements & Analyses Lab (RoMA, MPI-BGC) for their valuable lab analyses. We sincerely thank Carlos Alberto Quesada for his contributions and knowledge to this study. We also thank all the indigenous communities that have been bravely protecting the Amazon Forest and the people from riverside communities who have always worked together with us. Without the “mateiros”, we would never have achieved our scientific goals. Débora Pinheiro Oliveira was supported by the Coordination for the Improvement of Higher Education Personnel (CAPES), Brazilian Ministry of Education.

## **Financial support**

This research was supported by the National Institute for Amazonian Research (INPA), the Max Planck Institute for Biogeochemistry (MPI-BGC), and the ATTO project funded by the German Federal Ministry of Education and Research (BMBF grants 01LB1001A, 01LK1602, 01LK2101), the Brazilian Ministry of Science, Technology, Innovation and Communications (contract FINEP/MCTIC 01.11.01248.00), the Amazonas State University (UEA), the Amazonas Research Foundation (FAPEAM), LBA/INPA, and SDS/CEUC/RDS-Uatumã. Additional support was provided by the Deutsche Forschungsgemeinschaft (DFG project 352322796) and the PELD-MAUA project funded by CNPq/MCTI/CONFAP-FAPs (grant numbers 441811/2020-5 and



781 01.02.016301.02630/2022-76). D.P. Oliveira was supported by the Coordination for the  
782 Improvement of Higher Education Personnel (CAPES), Brazilian Ministry of Education.

## 783 References

784 Aaltonen, H., Pumpanen, J., Pihlatie, M., Hakola, H., Hellen, H., Kulmala, L., Vesala, T., and  
785 Bäck, J.: Boreal pine forest floor biogenic volatile organic compound emissions peak in early  
786 summer and autumn, *Agric. For. Meteorol.*, 151, 682–691,  
787 doi:10.1016/j.agrformet.2010.12.010, 2011

788 Abis, L., Loubet, B., Ciuraru, R., Lafouge, F., Houot, S., Nowak, V., Tripied, J., Dequiedt,  
789 S., Maron, P. A., and Sadet-Bourgeteau, S.: Reduced microbial diversity induces larger  
790 volatile organic compound emissions from soils. *Scientific Reports*, 10(1), 1–15.  
791 <https://doi.org/10.1038/s41598-020-63091-8>, 2020

792 Adeney, J. M., Christensen, N. L., Vicentini, A., and Cohn-Haft, M.: White-sand Ecosystems  
793 in Amazonia. *Biotropica*, 48(1), 7–23. <https://doi.org/10.1111/btp.12293>, 2016

794 Andreae, M. O., Acevedo, O. C., Araújo, A., Artaxo, P., Barbosa, C. G. G., Barbosa, H. M.  
795 J., Brito, J., Carbone, S., Chi, X., Cintra, B. B. L., da Silva, N. F., Dias, N. L., Dias-Júnior,  
796 C. Q., Ditas, F., Ditz, R., Godoi, A. F. L., Godoi, R. H. M., Heimann, M., Hoffmann, T., and  
797 Yáñez-Serrano, A. M.: The Amazon Tall Tower Observatory (ATTO) in the remote Amazon  
798 Basin: overview of first results from ecosystem ecology, meteorology, trace gas, and aerosol  
799 measurements. *Atmospheric Chemistry and Physics Discussions*, 15(8), 11599–11726.  
800 <https://doi.org/10.5194/acpd-15-11599-2015>, 2015

801 Asensio, D., Owen, S. M., Llusà, J., and Peñuelas, J.: The distribution of volatile isoprenoids  
802 in the soil horizons around *Pinus halepensis* trees. *Soil Biology and Biochemistry*, 40(12),  
803 2937–2947. <https://doi.org/10.1016/j.soilbio.2008.08.008>, 2008

804 Aprile, F., and Darwich, A. J.: Nutrients and water-forest interactions in an Amazon  
805 floodplain lake: an ecological approach. *Acta Limnologica Brasiliensia*, 25(2), 169–182.  
806 <https://doi.org/10.1590/S2179-975X2013000200008>, 2013

807 Bach, T. J., and Rohmer, M.: Isoprenoid synthesis in plants and microorganisms: new



- 808 concepts and experimental approaches, Springer, doi:10.1007/978-1-4614-4063-5, 2013.
- 809 Bachy, A., Aubinet, M., Amelynck, C., Schoon, N., Bodson, B., Moureaux, C., Delaplace,  
810 P., De Ligne, A., and Heinesch, B.: Methanol exchange dynamics between a temperate  
811 cropland soil and the atmosphere. *Atmospheric Environment*, 176, 229–239.  
812 <https://doi.org/10.1016/j.atmosenv.2017.12.016>, 2018
- 813 Baggesen, N. S., Davie-Martin, C. L., Seco, R., Holst, T., and Rinnan, R. Bidirectional  
814 Exchange of Biogenic Volatile Organic Compounds in Subarctic Heath Mesocosms During  
815 Autumn Climate Scenarios. *Journal of Geophysical Research: Biogeosciences*, 127(6).  
816 <https://doi.org/10.1029/2021JG006688>, 2022.
- 817 Bao, X., Zhou, W., Xu, L., Zheng, Z., Mu, Z., Llusà, J., Zeng, J., Zhang, Y., Asensio, D.,  
818 Yang, K., Yi, Z., Wang, X., and Peñuelas, J.: A meta-analysis on plant volatile organic  
819 compound emissions of different plant species and responses to environmental stress. *Front.*  
820 *Plant Sci.*, 318, 120886, <https://doi.org/10.1016/j.envpol.2022.120886>, 2023
- 821 Beauchamp, J., Herbig, J., Gutmann, R. and Hansel, A. On the use of Tedlar bags for breath-  
822 gas sampling and analysis, *J. Breath Res.*, 2, 046001, doi:10.1088/1752-7155/2/4/046001,  
823 2008.
- 824 Borges, S. H., Whittaker, A., and de Almeida, R. A. M.: Bird diversity in the Serra do Aracá  
825 region, northwestern Brazilian Amazon: Preliminary check-list with considerations on  
826 biogeography and conservation. *Zoologia*, 31, 343–360, [https://doi.org/10.1590/S1984-](https://doi.org/10.1590/S1984-46702014000400006)  
827 [46702014000400006](https://doi.org/10.1590/S1984-46702014000400006), 2014
- 828 Botía, S., Komiya, S., Marshall, J., Koch, T., Gałkowski, M., Lavric, J., Gomes-Alves, E.,  
829 Walter, D., Fisch, G., Pinho, D. M., Nelson, B. W., Martins, G., Luijkx, I. T., Koren, G.,  
830 Florentie, L., Carioca de Araújo, A., Sá, M., Andreae, M. O., Heimann, M., and Gerbig, C.:  
831 The CO<sub>2</sub> record at the Amazon Tall Tower Observatory: A new opportunity to study  
832 processes on seasonal and inter-annual scales. *Global Change Biology*, 28(2), 588–611.  
833 <https://doi.org/10.1111/gcb.15905>, 2022
- 834 Bourtsoukidis, E., Behrendt, T., Yañez-Serrano, A. M., Hellén, H., Diamantopoulos, E.,  
835 Catão, E., Ashworth, K., Pozzer, A., Quesada, C. A., Martins, D. L., Sá, M., Araujo, A., Brito,



- 836 J., Artaxo, P., Kesselmeier, J., Lelieveld, J., and Williams, J.: Strong sesquiterpene emissions  
837 from Amazonian soils. *Nature Communications*, 9(1), 1–11. [https://doi.org/10.1038/s41467-](https://doi.org/10.1038/s41467-018-04658-y)  
838 018-04658-y, 2018
- 839 Bridgham, S. D., Cadillo-Quiroz, H., Keller, J. K., and Zhuang, Q.: Methane emissions from  
840 wetlands: Biogeochemical, microbial, and modeling perspectives from local to global scales.  
841 *Global Change Biology*, 19(5), 1325–1346. <https://doi.org/10.1111/gcb.12131>, 2013
- 842 Brown, P., Watts, P., Märk, T. D., and Mayhew, C. A.: Proton transfer reaction mass  
843 spectrometry investigations on the effects of reduced electric field and reagent ion internal  
844 energy on product ion branching ratios for a series of saturated alcohols. *International Journal*  
845 *of Mass Spectrometry*, 294(2–3), 103–111. <https://doi.org/10.1016/j.ijms.2010.05.028>, 2010
- 846 Caetano Garcia, M.: Biogenic volatile organic compound (BVOC) emissions from  
847 decomposing leaf-litter in central Amazonia (Doctoral dissertation, National Institute for  
848 Amazonian Research Manaus), 2022
- 849 Cai, Z. C., Xing, G. X., Shen, G. Y., Xu, H., Yan, X. Y., Tsuruta, H., Yagi, K., and Minami,  
850 K.: Measurements of CH<sub>4</sub> and N<sub>2</sub>O emissions from rice paddies in Fengqiu, China. *Soil*  
851 *Science and Plant Nutrition*, 45(1), 1–13. <https://doi.org/10.1080/00380768.1999.10409320>,  
852 1999
- 853 Carrión, O., Pratscher, J., Curson, A. R., Williams, B. T., Rostant, W. G., Murrell, J. C., Todd,  
854 J. D., Carruthers, D. N., and Lee, T. S.: Diversifying Isoprenoid Platforms via Atypical  
855 Carbon Substrates and Non-model Microorganisms. *Frontiers in Microbiology*, 12.  
856 <https://doi.org/10.3389/fmicb.2021.791089>, 2021
- 857 Chadwick, K. D., and Asner, G. P.: Landscape evolution and nutrient rejuvenation reflected  
858 in Amazon forest canopy chemistry. *Ecol Lett*, 21: 978–988.  
859 <https://doi.org/10.1111/ele.12963>, 2018
- 860 Chen, Y., Ma, S., Jiang, H., Hu, Y., and Lu, X.: Influences of litter diversity and soil moisture  
861 on soil microbial communities in decomposing mixed litter of alpine steppe species.  
862 *Geoderma*, 377(March), 114577. <https://doi.org/10.1016/j.geoderma.2020.114577>, 2020



- 863 Chomel, M., Guittonny-Larchevêque, M., Fernandez, C., Gallet, C., DesRochers, A., Paré,  
864 D., Jackson, B. G., and Baldy, V.: Plant secondary metabolites: A key driver of litter  
865 decomposition and soil nutrient cycling. *J. Ecol.*, 104, 1527–1541,  
866 <https://doi.org/10.1111/1365-2745.12644>, 2016
- 867 Conrad, R: The global methane cycle: Recent advances in understanding the microbial  
868 processes involved. *Environmental Microbiology Reports*, 1(5), 285–292.  
869 <https://doi.org/10.1111/j.1758-2229.2009.00038.x>, 2009
- 870 Conrad, R: Methane production in soil environments— anaerobic biogeochemistry and  
871 microbial life between flooding and desiccation. *Microorganisms*, 8(6), 1–12.  
872 <https://doi.org/10.3390/microorganisms8060881>, 2020
- 873 Cornu, S., Ambrosi, J. P., Lucas, Y., and Fevrier, D.: A comparative study of the soil solution  
874 chemistry of two Amazonian forest soils (Central Amazonia, Brazil). In *Hydrology and Earth  
875 System Sciences* (Vol. 1, Issue 2, pp. 313–324). <https://doi.org/10.5194/hess-1-313-1997>,  
876 1997
- 877 Cornwell, W. K., Cornelissen, J. H. C., Amatangelo, K., Dorrepaal, E., Eviner, V. T., Godoy,  
878 O., Hobbie, S. E., Hoorens, B., Kurokawa, H., Pérez-Harguindeguy, N., Quested, H. M.,  
879 Santiago, L. S., Wardle, D. A., Wright, I. J., Aerts, R., Allison, S. D., Van Bodegom, P.,  
880 Brovkin, V., Chatain, A., and Westoby, M.: Plant species traits are the predominant control  
881 on litter decomposition rates within biomes worldwide. *Ecol. Lett.*, 11, 1065–1071,  
882 <https://doi.org/10.1111/j.1461-0248.2008.01219.x>, 2008
- 883 Costa, F. R. C., Schietti, J., Stark, S. C., and Smith, M. N.: The other side of tropical forest  
884 drought: do shallow water table regions of Amazonia act as large-scale hydrological refugia  
885 from drought? *New Phytologist*, 237(3), 714–733. <https://doi.org/10.1111/nph.17914>, 2023
- 886 de Gouw, J. A., Goldan, P. D., Warneke, C., Kuster, W. C., Roberts, J. M., Marchewka, M.,  
887 Bertman, S. B., Pszenny, A. A. P., and Keene, W. C.: Validation of proton transfer reaction-  
888 mass spectrometry (PTR-MS) measurements of gas-phase organic compounds in the  
889 atmosphere during the New England Air Quality Study (NEAQS) in 2002. *Journal of  
890 Geophysical Research D: Atmospheres*, 108(21), 1–18.



- 891 <https://doi.org/10.1029/2003jd003863>, 2023
- 892 de Mendonça, B. A. F., Filho, E. I. F., Schaefer, C. E. G. R., Simas, F. N. B., and de Paula,  
893 M. D.: Os solos das campinaranas na amazônia Brasileira: Ecossistemas arenícolas  
894 oligotróficos. *Ciencia Florestal*, 25(4), 827–839. <https://doi.org/10.5902/1980509820581>,  
895 2015
- 896 de Oliveira Marques, J. D., Luizão, F. J., Teixeira, W. G., Nogueira, E. M., Fearnside, P. M.,  
897 and Sarrazin, M.: Soil Carbon Stocks under Amazonian Forest: Distribution in the Soil  
898 Fractions and Vulnerability to Emission. *Open Journal of Forestry*, 07(02), 121–142.  
899 <https://doi.org/10.4236/ojf.2017.72008>, 2017
- 900 Demarchi, L. O., Klein, V. P., Aguiar, D. P. P., Marinho, L. C., Ferreira, M. J., Lopes, A., da  
901 Cruz, J., Quaresma, A. C., Schöngart, J., Wittmann, F., and Piedade, M. T. F.: The specialized  
902 white-sand flora of the Uatumã Sustainable Development Reserve, central Amazon, Brazil,  
903 Check List, 18, 187–217, <https://doi.org/10.15560/18.1.187>, 2022
- 904 Draper, F. C., Roucoux, K. H., Lawson, I. T., Mitchard, E. T. A., Honório Coronado, E. N.,  
905 Lähdenoja, O., Montenegro, L. T., Sandoval, E. V., Zarate, R., and Baker, T. R.: The  
906 distribution and amount of carbon in the largest peatland complex in Amazonia, *Environ.*  
907 *Res. Lett.*, 9, 124017, <https://doi.org/10.1088/1748-9326/9/12/124017>, 2014
- 908 Dixon, J. L., Hopkins, F. E., Stephens, J. A., and Schäfer, H.: Seasonal changes in microbial  
909 dissolved organic sulfur transformations in coastal waters, *Microorganisms*, 8, 337,  
910 <https://doi.org/10.3390/microorganisms8030337>, 2020
- 911 Dunne, E., Galbally, I. E., Lawson, S., and Patti, A.: Interference in the PTR-MS  
912 measurement of acetonitrile at  $m/z$  42 in polluted urban air—a study using switchable reagent  
913 ion PTR-MS, *Int. J. Mass Spectrom.*, 319–320, 40–47,  
914 <https://doi.org/10.1016/j.ijms.2012.05.004>, 2012
- 915 Durán, J., and Delgado-Baquerizo, M.: Vegetation structure determines the spatial variability  
916 of soil biodiversity across biomes, *Sci. Rep.*, 10, 1–7, [https://doi.org/10.1038/s41598-020-](https://doi.org/10.1038/s41598-020-78483-z)  
917 78483-z, 2020





- 918 Edtbauer, A., Pfannerstill, E. Y., Pires Florentino, A. P., Barbosa, C. G. G., Rodriguez-  
919 Caballero, E., Zannoni, N., Alves, R. P., Wolff, S., Tsokankunku, A., Aptroot, A., de Oliveira  
920 Sá, M., de Araújo, A. C., Sörgel, M., de Oliveira, S. M., Weber, B., and Williams, J.:  
921 Cryptogamic organisms are a substantial source and sink for volatile organic compounds in  
922 the Amazon region, *Commun. Earth Environ.*, 2, 1–10, [https://doi.org/10.1038/s43247-021-](https://doi.org/10.1038/s43247-021-00328-y)  
923 00328-y, 2021
- 924 Emidio, K., Martins, S. V., Antônio, C., and Soares, A.: Structure of 15 hectares permanent  
925 plots of terra firme dense forest in central Amazon, 01, 603–  
926 615, <https://doi.org/10.1590/0100-67622016000400004>, 2016.
- 927 Empresa Brasileira de Pesquisa Agropecuária. Manual de análise química de solos, plantas e  
928 fertilizantes, 2nd Edn., EMBRAPA, Brasília, 1999.
- 929 Eyice, Ö., Namura, M., Chen, Y., McGenity, T. J., and Murrell, J. C.: SIP metagenomics  
930 identifies uncultivated Methylophilaceae as dimethylsulphide degrading bacteria in soil and  
931 lake sediment, *ISME J.*, 9, 2336–2348, <https://doi.org/10.1038/ismej.2015.37>, 2015
- 932 Fan, J., Luo, R., McConkey, B. G., and Ziadi, N.: Effects of nitrogen deposition and litter  
933 layer management on soil CO<sub>2</sub>, N<sub>2</sub>O, and CH<sub>4</sub> emissions in a subtropical pine forestland, *Sci.*  
934 *Rep.*, 10, 1–11, <https://doi.org/10.1038/s41598-020-65952-8>, 2020
- 935 Fan, Y., Zhang, Y., Osborne, B., and Zou, J.: Global patterns of soil greenhouse gas fluxes in  
936 response to litter manipulation, *Cell Rep. Sustain.*, 1, 100003,  
937 <https://doi.org/10.1016/j.crsus.2023.100003>, 2024
- 938 Franco, W., and Dezzio, N.: Soils and soil-water regime in the terra-firme-caatinga forest  
939 complex near San Carlos de Rio Negro, state of Amazonas, Venezuela, *Interciencia*, 19, 305–  
940 316, 1994.
- 941 Fine, P. V. A., and Baraloto, C.: Habitat endemism in white-sand forests: insights into the  
942 mechanisms of lineage diversification and community assembly of the Neotropical flora,  
943 *Biotropica*, 48, 24–33, <https://doi.org/10.1111/btp.12301>, 2016.
- 944 Fine, P. V. A., Miller, Z. J., Mesones, I., Irazuzta, S., Appel, H. M., Stevens, M. H. H.,



- 945 Sääksjärvi, I., Schultz, J. C., and Coley, P. D.: The growth-defense trade-off and habitat  
946 specialization by plants in Amazonian forests, *Ecology*, 87, 150–162,  
947 <https://doi.org/10.1126/science.1098982>, 2006
- 948 Flint, A. L., and Flint, L. E.: Particle density, in: *Methods of Soil Analysis, Part 4: Physical*  
949 *Methods*, 229–240. <https://doi.org/10.2136/sssabookser5.4.c10>, 2018
- 950 Flores, B. M., and Holmgren, M.: White-sand savannas expand at the core of the Amazon  
951 after forest wildfires, *Ecosystems*, 24, 1624–1637, [https://doi.org/10.1007/s10021-021-](https://doi.org/10.1007/s10021-021-00607-x)  
952 [00607-x](https://doi.org/10.1007/s10021-021-00607-x), 2021
- 953 Freschet, G. T., Aerts, R., and Cornelissen, J. H. C.: A plant economics spectrum of litter  
954 decomposability, *Funct. Ecol.*, 26, 56–65, <https://doi.org/10.1111/j.1365-2435.2011.01913.x>,  
955 2012
- 956 García-Villacorta, R., Dexter, K. G., and Pennington, T.: Amazonian white-sand forests show  
957 strong floristic links with surrounding oligotrophic habitats and the Guiana Shield,  
958 *Biotropica*, 48, 47–57, <https://doi.org/10.1111/btp.12302>, 2016
- 959 Gfeller, A., Laloux, M., Barsics, F., Kati, D. E., Haubruge, E., du Jardin, P., Verheggen, F.  
960 J., Lognay, G., Wathelet, J. P., and Fauconnier, M. L.: Characterization of volatile organic  
961 compounds emitted by barley (*Hordeum vulgare* L.) roots and their attractiveness to  
962 wireworms, *J. Chem. Ecol.*, 39, 1129–1139, <https://doi.org/10.1007/s10886-013-0302-3>,  
963 2013
- 964 Gomes Alves, E., Taylor, T., Robin, M., Pinheiro Oliveira, D., Schiatti, J., Duvoisin Júnior,  
965 S., Zannoni, N., Williams, J., Hartmann, C., Gonçalves, J. F. C., Schöngart, J., Wittmann, F.,  
966 and Piedade, M. T. F.: Seasonal shifts in isoprenoid emission composition from three  
967 hyperdominant tree species in central Amazonia, *Plant Biol.*, 24, 721–733, Seasonal shifts in  
968 isoprenoid emission composition from three hyperdominant tree species in central Amazonia.  
969 *Plant Biology*, 24(5), 721–733. <https://doi.org/10.1111/plb.13419>, 2022
- 970 Greenberg, J. P., Asensio, D., Turnipseed, A., Guenther, A. B., Karl, T., and Gochis, D.:  
971 Contribution of leaf and needle litter to whole ecosystem BVOC fluxes, *Atmos. Environ.*, 59,  
972 302–311, <https://doi.org/10.1016/j.atmosenv.2012.04.038>, 2012



- 973 Guenther, A. B., Jiang, X., Heald, C. L., Sakulyanontvittaya, T., Duhl, T., Emmons, L. K.,  
974 and Wang, X.: The model of emissions of gases and aerosols from nature version 2.1  
975 (MEGAN2.1): an extended and updated framework for modeling biogenic emissions, *Geosci.*  
976 *Model Dev.*, 5, 1471–1492, <https://doi.org/10.5194/gmd-5-1471-2012>, 2012
- 977 Hair, J. F., Black, W. C., Babin, B. J. and Anderson, R. E. *Multivariate data analysis*, 7th  
978 Edn., Pearson, Upper Saddle River, 2009.
- 979 Hernandez-Arranz, S., Perez-Gil, J., Marshall-Sabey, D., and Rodriguez-Concepcion, M.:  
980 Engineering *Pseudomonas putida* for isoprenoid production by manipulating endogenous and  
981 shunt pathways supplying precursors, *Microb. Cell Fact.*, 18, 1–14,  
982 <https://doi.org/10.1186/s12934-019-1204-z>, 2019
- 983 Hofmann, K., Pauli, H., Praeg, N., Wagner, A. O., and Illmer, P.: Methane-cycling  
984 microorganisms in soils of a high-alpine altitudinal gradient, *FEMS Microbiol. Ecol.*, 92,  
985 fiw009, <https://doi.org/10.1093/femsec/fiw009>, 2016
- 986 Huangfu, Y., Yuan, B., Wang, S., Wu, C., He, X., Qi, J., de Gouw, J., Warneke, C., Gilman,  
987 J. B., Wisthaler, A., Karl, T., Graus, M., Jobson, B. T., and Shao, M.: Revisiting acetonitrile  
988 as tracer of biomass burning in anthropogenic-influenced environments, *Geophys. Res. Lett.*,  
989 48, e2020GL092322, <https://doi.org/10.1029/2020GL092322>, 2021
- 990 Jardine, K., Yáñez-Serrano, A. M., Williams, J., Kunert, N., Jardine, A., Taylor, T., Abrell,  
991 L., et al.: Dimethyl sulfide in the Amazon rainforest, *Glob. Biogeochem. Cycles*, 29, 19–32,  
992 <https://doi.org/10.1002/2014GB004969>, 2015
- 993 Jdanova, M., and Isidorov, V.: Volatile organic compounds from leaves litter, *Chemosphere*,  
994 48, 2058–2072, doi:10.1016/S0045-6535(02)00365-7, 2002.
- 995 Jenkinson, D. S., Brookes, P. C., and Powlson, D. S.: Measuring soil microbial biomass, *Soil*  
996 *Biol. Biochem.*, 36, 5–7, <https://doi.org/10.1016/j.soilbio.2003.10.002>, 2004
- 997 Jiao, Y., Kramshøj, M., Davie-Martin, C. L., Albers, C. N., and Rinnan, R.: Soil uptake of  
998 VOCs exceeds production when VOCs are readily available, *Soil Biol. Biochem.*, 185,  
999 109153, <https://doi.org/10.1016/j.soilbio.2023.109153>, 2023



- 1000 Kuzma, J., Nemecek-Marshall, M., Pollock, W. H., and Fall, R.: Bacteria produce the volatile  
1001 hydrocarbon isoprene, *Curr. Microbiol.*, 30, 97–103, <https://doi.org/10.1007/BF00294190>,  
1002 1995
- 1003 Lamers, L. P., Govers, L. L., Janssen, I. C., Geurts, J. J., Van der Welle, M. E., Van Katwijk,  
1004 M. M., Smolders, A. J.: Sulfide as a soil phytotoxin—a review, *Front. Plant Sci.*, 4, 268,  
1005 <https://doi.org/10.3389/fpls.2013.00268>, 2013
- 1006 Lee, J., Oh, Y., Lee, S. T., Seo, Y. O., Yun, J., Yang, Y., Kim, J., Zhuang, Q., and Kang, H.:  
1007 Soil organic carbon is a key determinant of CH<sub>4</sub> sink in global forest soils, *Nat. Commun.*,  
1008 14, 6–13, <https://doi.org/10.1038/s41467-023-38905-8>, 2023
- 1009 Leff, J. W., and Fierer, N.: Volatile organic compound (VOC) emissions from soil and litter  
1010 samples, *Soil Biol. Biochem.*, 40, 1629–1636, <https://doi.org/10.1016/j.soilbio.2008.01.018>,  
1011 2008
- 1012 Lehnert, A. S., Cooper, R. E., Ignatz, R., Ruecker, A., Gomes-Alves, E., Küsel, K., Pohnert,  
1013 G., and Trumbore, S. E.: Dimethyl sulfide emissions from a peatland result more from organic  
1014 matter degradation than sulfate reduction, *J. Geophys. Res. Biogeosci.*, 129, e2023JG007449,  
1015 <https://doi.org/10.1029/2023JG007449>, 2024
- 1016 Li Q, Hu W, Li L, Li Y. Interactions between organic matter and Fe oxides at soil micro-  
1017 interfaces: Quantification, associations, and influencing factors. *Sci Total Environ.* 2023 Jan  
1018 10;855:158710. doi: 10.1016/j.scitotenv.2022.158710
- 1019 Lin, C., Owen, S. M., and Peñuelas, J.: Volatile organic compounds in the roots and  
1020 rhizosphere of *Pinus* spp., *Soil Biol. Biochem.*, 39, 951–960,  
1021 <https://doi.org/10.1016/j.soilbio.2006.11.007>, 2007
- 1022 Lindinger, W., Hansel, A., and Jordan, A.: On-line monitoring of volatile organic compounds  
1023 at pptv levels by means of proton-transfer-reaction mass spectrometry (PTR-MS) medical  
1024 applications, food control and environmental research, *Int. J. Mass Spectrom. Ion Process.*,  
1025 173, 191–241, [https://doi.org/10.1016/s0168-1176\(97\)00281-4](https://doi.org/10.1016/s0168-1176(97)00281-4), 1998
- 1026 Liu, Y., Ciuraru, R., Abis, L., Amelynck, C., Buysse, P., Guenther, A., Heinesch, B., Lafouge,



- 1027 F., Levvasseur, F., Loubet, B., Voyard, A., and Massad, R.-S.: Emissions of biogenic volatile  
1028 organic compounds from agricultural lands and the impact of land-use and other management  
1029 practices: a review, *EGUsphere* [preprint], 1–35, [https://doi.org/10.5194/egusphere-2024-](https://doi.org/10.5194/egusphere-2024-530)  
1030 530, 2024
- 1031 Llusà, J., Asensio, D., Sardans, J., Filella, I., Peguero, G., Grau, O., Ogaya, R., Gargallo-  
1032 Garriga, A., Verryckt, L. T., Van Langenhove, L., Brechet, L. M., Courtois, E., Stahl, C.,  
1033 Janssens, I. A., and Peñuelas, J.: Contrasting nitrogen and phosphorus fertilization effects on  
1034 soil terpene exchanges in a tropical forest, *Sci. Total Environ.*, 802,  
1035 149769, <https://doi.org/10.1016/j.scitotenv.2021.149769>, 2022
- 1036 Luize, B. G., Magalhães, J. L. L., Queiroz, H., Lopes, M. A., Venticinque, E. M., de Moraes  
1037 Novo, E. M. L., and Silva, T. S. F.: The tree species pool of Amazonian wetland forests:  
1038 which species can assemble in periodically waterlogged habitats?, *PLoS ONE*, 13, e0198130,  
1039 <https://doi.org/10.1371/journal.pone.0198130>, 2018
- 1040 Venturini, A. M., Gontijo, J. B., Mandro, J. A., Berenguer, E., Peay, K. G., Tsai, S. M., and  
1041 Bohannon, B. J. M.: Soil microbes under threat in the Amazon rainforest, *Trends Ecol. Evol.*,  
1042 38, 693–696, <https://doi.org/10.1016/j.tree.2023.04.014>, 2023
- 1043 Mäki, M., Heinonsalo, J., Hellén, H., and Bäck, J.: Contribution of understorey vegetation  
1044 and soil processes to boreal forest isoprenoid exchange, *Biogeosciences*, 14, 1055–1073,  
1045 <https://doi.org/10.5194/bg-14-1055-2017>, 2017
- 1046 Mancuso, S., Taiti, C., Bazihizina, N., Costa, C., Menesatti, P., Giagnoni, L., Arenella, M.,  
1047 Nannipieri, P., and Renella, G.: Soil volatile analysis by proton transfer reaction-time of flight  
1048 mass spectrometry (PTR-TOF-MS), *Appl. Soil Ecol.*, 86, 182–191,  
1049 <https://doi.org/10.1016/j.apsoil.2014.10.018>, 2015
- 1050 Mazahar, S., and Umar, S.: Soil potassium availability and role of microorganisms in  
1051 influencing potassium availability to plants, in: *Role of potassium in abiotic stress*, 77–87,  
1052 [https://doi.org/10.1007/978-981-16-4461-0\\_4](https://doi.org/10.1007/978-981-16-4461-0_4), 2022
- 1053 McGenity, T. J., Crombie, A. T., and Murrell, J. C.: Microbial cycling of isoprene, the most  
1054 abundantly produced biological volatile organic compound on Earth, *ISME J.*, 12, 931–941,



- 1055 <https://doi.org/10.1038/s41396-018-0072-6>, 2018
- 1056 Miyama, T., Morishita, T., Kominami, Y., Noguchi, H., Yasuda, Y., Yoshifuji, N., Okano,  
1057 M., Yamanoi, K., Mizoguchi, Y., Takanashi, S., Kitamura, K., and Matsumoto, K.: Increases  
1058 in biogenic volatile organic compound concentrations observed after rains at six forest sites  
1059 in non-summer periods, *Atmosphere*, 11, 13181, <https://doi.org/10.3390/atmos11121381>,  
1060 2020
- 1061 Monard, C., Caudal, J. P., Cluzeau, D., Le Garrec, J. L., Hellequin, E., Hoeffner, K., Humbert,  
1062 G., Jung, V., Le Lann, C., and Nicolai, A.: Short-term temporal dynamics of VOC emissions  
1063 by soil systems in different biotopes, *Front. Environ. Sci.*, 9, 650701,  
1064 <https://doi.org/10.3389/fenvs.2021.650701>, 2021
- 1065 Mosquera, Q. H.; Torres-Torres, J.J.; Pérez-Abadía, D. Influence of Mining on Nutrient  
1066 Cycling in the Tropical Rain Forests of the Colombian Pacific. *Forests* 2024, 15, 1222.  
1067 <https://doi.org/10.3390/f15071222>
- 1068 Mu, Z., Llusà, J., Zeng, J., Zhang, Y., Asensio, D., Yang, K., Yi, Z., Wang, X., and Peñuelas,  
1069 J.: An overview of the isoprenoid emissions from tropical plant species, *Front. Plant Sci.*, 13,  
1070 833030, <https://doi.org/10.3389/fpls.2022.833030>, 2022
- 1071 Murphy, J., and Riley, J. P.: A modified single solution method for the determination of  
1072 phosphate in natural waters, *Anal. Chim. Acta*, 27, 31–36, [https://doi.org/10.1016/S0003-](https://doi.org/10.1016/S0003-2670(00)88444-5)  
1073 [2670\(00\)88444-5](https://doi.org/10.1016/S0003-2670(00)88444-5), 1962
- 1074 Murrell, J. C., McGenity, T. J., and Crombie, A. T.: Microbial metabolism of isoprene: a  
1075 much-neglected climate-active gas, *Microbiology*, 166, 600–613,  
1076 <https://doi.org/10.1099/mic.0.000931>, 2020
- 1077 Ndah, F., Valolahti, H., Schollert, M., Michelsen, A., and Kivimäenpää, M.: Influence of  
1078 increased nutrient availability on biogenic volatile organic compound (BVOC) emissions and  
1079 leaf anatomy of subarctic dwarf shrubs under climate warming and increased cloudiness,  
1080 *Ann. Bot.*, 129, 443–455, doi:10.1093/aob/mcac004, 2022.
- 1081 Oliveira-Filho, A. T., Dexter, K. G., Pennington, R. T., Simon, M. F., Bueno, M. L., and



- 1082 Neves, D. M.: On the floristic identity of Amazonian vegetation types, *Biotropica*, 53, 767–  
1083 777, <https://doi.org/10.1093/aob/mcac004>, 2021
- 1084 Onwuka, B.: Effects of soil temperature on some soil properties and plant growth, *Adv. Plants*  
1085 *Agric. Res.*, 8, 34–37, <https://doi.org/10.15406/apar.2018.08.00288>, 2018
- 1086 Package, T. *olsrr: tools for building OLS regression models*, R package version 0.5.3, [cran.r-](https://cran.r-project.org)  
1087 [project.org](https://cran.r-project.org), 2024.
- 1088 Peñuelas, J., and Staudt, M.: BVOCs and global change, *Trends Plant Sci.*, 15, 133–144,  
1089 <https://doi.org/10.1016/j.tplants.2009.12.005>, 2010
- 1090 Peñuelas, J., Asensio, D., Tholl, D., Wenke, K., Rosenkranz, M., Piechulla, B., and  
1091 Schnitzler, J. P.: Biogenic volatile emissions from the soil, *Plant Cell Environ.*, 37, 1866–  
1092 1891, <https://doi.org/10.1111/pce.12340>, 2014
- 1093 Pugliese, G., Ingrisch, J., Meredith, L. K., Pfannerstill, E. Y., Klüpfel, T., Meeran, K., Byron,  
1094 J., Purser, G., Gil-Loaiza, J., van Haren, J., Dontsova, K., Kreuzwieser, J., Ladd, S. N.,  
1095 Werner, C., and Williams, J.: Effects of drought and recovery on soil volatile organic  
1096 compound fluxes in an experimental rainforest, *Nat. Commun.*, 14, 40661,  
1097 <https://doi.org/10.1038/s41467-023-40661-8>, 2023
- 1098 Pulido, P., Perello, C., and Rodriguez-Concepcion, M.: New insights into plant isoprenoid  
1099 metabolism, *Mol. Plant*, 5, 964–967, <https://doi.org/10.1093/mp/sss088>, 2012
- 1100 Quesada, C. A., Lloyd, J., Schwarz, M., Baker, T. R., Phillips, O. L., Patiño, S., Czimczik,  
1101 C., Hodnett, M. G., Herrera, R., Arneeth, A., Lloyd, G., Malhi, Y., Dezzio, N., Luizão, F. J.,  
1102 Santos, A. J. B., Schmerler, J., Arroyo, L., Silveira, M., Priante Filho, N., and Ramírez, H.:  
1103 Regional and large-scale patterns in Amazon forest structure and function are mediated by  
1104 variations in soil physical and chemical properties, *Biogeosciences Discuss.*, 6, 3993–4057,  
1105 <https://doi.org/10.5194/bgd-6-3993-2009>, 2009
- 1106 Quesada, C. A., Lloyd, J., Anderson, L. O., Fyllas, N. M., Schwarz, M., and Czimczik, C. I.:  
1107 Soils of Amazonia with particular reference to the RAINFOR sites, *Biogeosciences*, 8, 1415–  
1108 1440, <https://doi.org/10.5194/bg-8-1415-2011>, 2011





- 1109 Quesada, C. A., Phillips, O. L., Schwarz, M., Czimeczik, C. I., Baker, T. R., Patiño, S., Fyllas,  
1110 N. M., Hodnett, M. G., Herrera, R., Almeida, S., Alvarez Dávila, E., Arneth, A., Arroyo, L.,  
1111 Chao, K. J., Dezzio, N., Erwin, T., Di Fiore, A., Higuchi, N., Honorio Coronado, E., and  
1112 Lloyd, J.: Basin-wide variations in Amazon forest structure and function are mediated by both  
1113 soils and climate, *Biogeosciences*, 9, 2203–2246, <https://doi.org/10.5194/bg-9-2203-2012>,  
1114 2012
- 1115 Rasheed, M. U., Kivimäenpää, M., and Kasurinen, A.: Emissions of biogenic volatile organic  
1116 compounds (BVOCs) from the rhizosphere of Scots pine (*Pinus sylvestris*) seedlings exposed  
1117 to warming, moderate N addition and bark herbivory by large pine weevil (*Hylobius abietis*),  
1118 *Plant Soil*, 463, 379–394, <https://doi.org/10.1007/s11104-021-04888-y>, 2021
- 1119 Raza, W., Mei, X., Wei, Z., Ling, N., Yuan, J., Wang, J., Huang, Q., and Shen, Q.: Profiling  
1120 of soil volatile organic compounds after long-term application of inorganic, organic and  
1121 organic-inorganic mixed fertilizers and their effect on plant growth, *Sci. Total Environ.*, 607–  
1122 608, 326–338, <https://doi.org/10.1016/j.scitotenv.2017.07.023>, 2017
- 1123 Ringsdorf, A., Edtbauer, A., Holanda, B., Poehlker, C., Sá, M. O., Araújo, A., Kesselmeier,  
1124 J., Lelieveld, J., and Williams, J.: Investigating carbonyl compounds above the Amazon  
1125 rainforest using PTR-ToF-MS with NO<sup>+</sup> chemical ionization, *EGUsphere* [preprint],  
1126 <https://doi.org/10.5194/egusphere-2024-1210>, 2024
- 1127 Rinnan, R., Gierth, D., Bilde, M., Rosenørn, T., and Michelsen, A.: Off-season biogenic  
1128 volatile organic compound emissions from heath mesocosms: responses to vegetation cutting,  
1129 *Front. Microbiol.*, 4, 224, <https://doi.org/10.3389/fmicb.2013.00224>, 2013
- 1130 Rodrigues, P. M. S., Schaefer, C. E. G. R., De Oliveira Silva, J., Ferreira, W. G., Dos Santos,  
1131 R. M., and Neri, A. V.: The influence of soil on vegetation structure and plant diversity in  
1132 different tropical savannic and forest habitats, *J. Plant Ecol.*, 11, 226–236,  
1133 <https://doi.org/10.1093/jpe/rtw135>, 2018
- 1134 Rosace, M. C., Veronesi, F., Briggs, S., Cardenas, L. M., and Jeffery, S.: Legacy effects  
1135 override soil properties for CO<sub>2</sub> and N<sub>2</sub>O but not CH<sub>4</sub> emissions following digestate  
1136 application to soil, *GCB Bioenergy*, 12, 445–457, <https://doi.org/10.1111/gcbb.12688>, 2020



- 1137 Rossetti, D. F., Moulatlet, G. M., Tuomisto, H., Gribel, R., Toledo, P. M., Valeriano, M. M.,  
1138 Ruokolainen, K., Cohen, M. C. L., Cordeiro, C. L. O., Rennó, C. D., Coelho, L. S., and  
1139 Ferreira, C. A. C.: White sand vegetation in an Amazonian lowland under the perspective of  
1140 a young geological history, *An. Acad. Bras. Cienc.*, 91, e20181337,  
1141 <https://doi.org/10.1590/0001-3765201920181337>, 2019
- 1142 Sanhueza, E., Holzinger, R., Kleiss, B., Donoso, L., and Crutzen, P. J.: New insights in the  
1143 global cycle of acetonitrile: release from the ocean and dry deposition in the tropical savanna  
1144 of Venezuela, *Atmos. Chem. Phys.*, 4, 275–280, <https://doi.org/10.5194/acp-4-275-2004>,  
1145 2004
- 1146 Saunier, A., Mpamah, P., Biasi, C., and Blande, J. D.: Microorganisms in the phylloplane  
1147 modulate the BVOC emissions of *Brassica nigra* leaves, *Plant Signal. Behav.*, 15, 1728468,  
1148 <https://doi.org/10.1080/15592324.2020.1728468>, 2020
- 1149 Schade, G. W., and Goldstein, A. H.: Fluxes of oxygenated volatile organic compounds from  
1150 a ponderosa pine plantation, *J. Geophys. Res. Atmos.*, 106, 3111–3123,  
1151 <https://doi.org/10.1029/2000JD900592>, 2001
- 1152 Schindler, T., Mander, Ü., Machacova, K., Espenberg, M., Krasnov, D., Escuer-Gatius, J.,  
1153 Veber, G., Pärn, J., and Soosaar, K.: Short-term flooding increases CH<sub>4</sub> and N<sub>2</sub>O emissions  
1154 from trees in a riparian forest soil-stem continuum, *Sci. Rep.*, 10, 60058,  
1155 <https://doi.org/10.1038/s41598-020-60058-7>, 2020
- 1156 Shah, A., Huang, J., Han, T., Khan, M. N., Tadesse, K. A., Daba, N. A., Khan, S., Ullah, S.,  
1157 Sardar, M. F., Fahad, S., and Zhang, H.: Impact of soil moisture regimes on greenhouse gas  
1158 emissions, soil microbial biomass, and enzymatic activity in long-term fertilized paddy soil,  
1159 *Environ. Sci. Eur.*, 36, 943, <https://doi.org/10.1186/s12302-024-00943-4>, 2024
- 1160 Sharkey, T. D., and Monson, R. K.: Isoprene research – 60 years later, the biology is still  
1161 enigmatic, *Plant Cell Environ.*, 40, 1671–1678, <https://doi.org/10.1111/pce.12930>, 2017
- 1162 Sillo, F., Neri, L., Calvo, A., Zampieri, E., Petruzzelli, G., Ferraris, I., Delledonne, M., Zaldei,  
1163 A., Gioli, B., Baraldi, R., and Balestrini, R.: Correlation between microbial communities and  
1164 volatile organic compounds in an urban soil provides clues on soil quality towards



- 1165 sustainability of city flowerbeds, *Heliyon*, 10, e23594,  
1166 <https://doi.org/10.1016/j.heliyon.2023.e23594>, 2024
- 1167 Simon, C., Pimentel, T. P., Monteiro, M. T. F., Candido, L. A., Gastmans, D., Geilmann, H.,  
1168 ... & Gleixner, G.: Molecular links between whitesand ecosystems and blackwater formation  
1169 in the Rio Negro watershed. *Geochimica et Cosmochimica Acta*, 311, 274–291.  
1170 <https://doi.org/10.1016/j.gca.2021.06.036>, 2021
- 1171 Steeghs, M., Bais, H. P., de Gouw, J., Goldan, P., Kuster, W., Northway, M., Fall, R., and  
1172 Vivanco, J. M.: Proton-transfer-reaction mass spectrometry as a new tool for real time  
1173 analysis of root-secreted volatile organic compounds in *Arabidopsis*, *Plant Physiol.*, 135, 47–  
1174 58, <https://doi.org/10.1104/pp.104.038703>, 2004
- 1175 Stotzky, G., Schenck, S., and Papavizas, G. C.: Volatile organic compounds and  
1176 microorganisms, *Crit. Rev. Microbiol.*, 4, 333–382,  
1177 <https://doi.org/10.3109/10408417609102303>, 1976
- 1178 Stropp, J., Van der Sleen, P., Assunção, P. A., Silva, A. L., and ter Steege, H.: Tree  
1179 communities of white-sand and terra-firme forests of the upper Rio Negro, *Acta Amazon.*,  
1180 41, 521–544, <https://doi.org/10.1590/s0044-59672011000400010>, 2011
- 1181 Svendsen, S. H., Lindwall, F., Michelsen, A., and Rinnan, R.: Biogenic volatile organic  
1182 compound emissions along a high arctic soil moisture gradient, *Sci. Total Environ.*, 573, 131–  
1183 138, <https://doi.org/10.1016/j.scitotenv.2016.08.100>, 2016
- 1184 Souza, J. J. L. L., Fontes, M. P. F., Gilkes, R., Costa, L. M., and Oliveira, T. S.: Geochemical  
1185 signature of Amazon tropical rainforest soils, *Rev. Bras. Cienc. Solo*, 42, e0170192,  
1186 <https://doi.org/10.1590/18069657rbcs20170192>, 2018
- 1187 Tang, J., Schurgers, G., and Rinnan, R.: Process understanding of soil BVOC fluxes in natural  
1188 ecosystems: a review, *Rev. Geophys.*, 57, 966–986, <https://doi.org/10.1029/2018RG000634>,  
1189 2019
- 1190 Targhetta, N., Kesselmeier, J., and Wittmann, F.: Effects of the hydroedaphic gradient on tree  
1191 species composition and aboveground wood biomass of oligotrophic forest ecosystems in the



- 1192 central Amazon basin, *Folia Geobot.*, 50, 185–205, <https://doi.org/10.1007/s12224-015->  
1193 9225-9, 2015
- 1194 ter Steege, H., Pitman, N. C. A., Sabatier, D., Baraloto, C., Salomão, R. P., Guevara, J. E.,  
1195 Phillips, O. L., Castilho, C. V., Magnusson, W. E., Molino, J. F., Monteagudo, A., Vargas, P.  
1196 N., Montero, J. C., Feldpausch, T. R., Coronado, E. N. H., Killeen, T. J., Mostacedo, B.,  
1197 Vasquez, R., Assis, R. L., and Silman, M. R.: Hyperdominance in the Amazonian tree flora,  
1198 *Science*, 342, 1243092, <https://doi.org/10.1126/science.1243092>, 2013
- 1199 Thulasiram, H. V., Erickson, H. K., and Poulter, C. D.: Chimeras of two isoprenoid synthases  
1200 catalyze all four coupling reactions in isoprenoid biosynthesis, *Science*, 316, 73–76,  
1201 <https://doi.org/10.1126/science.1137786>, 2007
- 1202 Trowbridge, A. M., Stoy, P. C., and Phillips, R. P.: Soil biogenic volatile organic compound  
1203 flux in a mixed hardwood forest: net uptake at warmer temperatures and the importance of  
1204 mycorrhizal associations, *J. Geophys. Res. Biogeosci.*, 125, e2019JG005479,  
1205 <https://doi.org/10.1029/2019JG005479>, 2020
- 1206 van Asperen, H., Warneke, T., Carioca de Araújo, A., Rider Forsberg, B., Ramos de Oliveira,  
1207 L., de Lima Xavier, T., de Oliveira Sá, M., Ricardo Teixeira, P., Azevedo de Oliveira, R.,  
1208 Sousa de Moura, V., do Socorro Monteiro Leal, L., Botia, S., Lavrič, J., Komiya, S., Frumau,  
1209 A., Hensen, A., van den Bulk, P., van Dinter, D., and Notholt, J.: Tropical forest CH<sub>4</sub>: from  
1210 flux chambers to micrometeorological tower measurements, *EGU General Assembly 2020*,  
1211 Online, 4–8 May 2020, EGU2020-6139, <https://doi.org/10.5194/egusphere-egu2020-6139>,  
1212 2020
- 1213 Van Den Pol-van Dasselaar, A., Van Beusichem, M. L., and Oenema, O.: Effects of soil  
1214 moisture content and temperature on methane uptake by grasslands on sandy soils, *Plant Soil*,  
1215 204, 213–222, <https://doi.org/10.1023/A:1004371309361>, 1998
- 1216 Vermeuel, M. P., Novak, G. A., Kilgour, D. B., Claflin, M. S., Lerner, B. M., Trowbridge, A.  
1217 M., Thom, J., Cleary, P. A., Desai, A. R., and Bertram, T. H.: Observations of biogenic  
1218 volatile organic compounds over a mixed temperate forest during the summer to autumn  
1219 transition, *Atmos. Chem. Phys.*, 23, 4123–4148, <https://doi.org/10.5194/acp-23-4123-2023>,



- 1220 2023
- 1221 Viros, J., Santonja, M., Temime-Roussel, B., Wortham, H., Fernandez, C., and Ormeño, E.:  
1222 Volatilome of Aleppo pine litter over decomposition process, *Ecol. Evol.*, 11, 6862–6880,  
1223 <https://doi.org/10.1002/ece3.7533>, 2021
- 1224 Vlasenko, A., MacDonald, A. M., Sjostedt, S. J., and Abbatt, J. P. D.: Formaldehyde  
1225 measurements by proton transfer reaction–mass spectrometry (PTR-MS): correction for  
1226 humidity effects, *Atmos. Meas. Tech.*, 3, 1055–1062, [https://doi.org/10.5194/amt-3-1055-](https://doi.org/10.5194/amt-3-1055-2010)  
1227 2010, 2010
- 1228 Yáñez-Serrano, A. M., Filella, I., Llusà, J., Gargallo-Garriga, A., Granda, V., Bourtsoukidis,  
1229 E., Peñuelas, J., et al.: GLOVOCS-master compound assignment guide for proton transfer  
1230 reaction mass spectrometry users, *Atmos. Environ.*, 244, 117929,  
1231 <https://doi.org/10.1016/j.atmosenv.2020.117929>, 2021
- 1232 Wachiye, S., Merbold, L., Vesala, T., Rinne, J., Räsänen, M., Leitner, S., and Pellikka, P.:  
1233 Soil greenhouse gas emissions under different land-use types in savanna ecosystems of  
1234 Kenya, *Biogeosciences*, 17, 2149–2167, <https://doi.org/10.5194/bg-17-2149-2020>, 2020
- 1235 Wang, M., Zheng, Q., Shen, Q., and Guo, S.: The critical role of potassium in plant stress  
1236 response, *Int. J. Mol. Sci.*, 14, 7370–7390, <https://doi.org/10.3390/ijms14047370>, 2013
- 1237 Warneke, C., Karl, T., Judmaier, H., Hansel, A., Jordan, A., Lindinger, W., and Crutzen, P.  
1238 J.: Acetone, methanol, and other partially oxidized volatile organic emissions from dead plant  
1239 matter by abiological processes: significance for atmospheric HO(X) chemistry, *Glob.*  
1240 *Biogeochem. Cycles*, 13, 9–17, <https://doi.org/10.1029/98GB02428>, 1999
- 1241 Warneke, C., Veres, P., Murphy, S. M., Soltis, J., Field, R. A., Graus, M. G., Koss, A., Li, S.  
1242 M., Li, R., Yuan, B., Roberts, J. M., and de Gouw, J. A.:
- 1243 PTR-QMS versus PTR-TOF comparison in a region with oil and natural gas extraction  
1244 industry in the Uintah Basin in 2013, *Atmos. Meas. Tech.*, 8, 411–420,  
1245 <https://doi.org/10.5194/amt-8-411-2015>, 2015
- 1246 Wells, K. C., Millet, D. B., Payne, V. H., Vigouroux, C., Aquino, C. A. B., De Mazière, M.,



- 1247 de Gouw, J. A., Graus, M., Kurosu, T., Warneke, C., and Wisthaler, A.: Next-generation  
1248 isoprene measurements from space: detecting daily variability at high resolution, *J. Geophys.*  
1249 *Res. Atmos.*, 127, e2021JD036181, <https://doi.org/10.1029/2021JD036181>, 2022
- 1250 Williams, J., Pöschl, U., Crutzen, P. J., Hansel, A., Holzinger, R., Warneke, C., Lindinger,  
1251 W., and Lelieveld, J.: An atmospheric chemistry interpretation of mass scans obtained from  
1252 a proton transfer mass spectrometer flown over the tropical rainforest of Surinam, *J. Atmos.*  
1253 *Chem.*, 38, 133–166, <https://doi.org/10.1023/A:10063227015232001>, 2001.
- 1254 Zanchi, F. B., Waterloo, M. J., Tapia, A. P., Alvarado Barrientos, M. S., Bolson, M. A.,  
1255 Luizão, F. J., Manzi, A. O., and Dolman, A. J.: Igapó (black-water flooded forests) of the  
1256 Amazon Basin, in: *The Amazon: Limnology and landscape ecology of a mighty tropical river*  
1257 *and its basin*, edited by: Sioli, H., Springer, Cham, 59–66, [https://doi.org/10.1007/978-3-319-](https://doi.org/10.1007/978-3-319-90122-0_7)  
1258 [90122-0\\_7](https://doi.org/10.1007/978-3-319-90122-0_7), 2018.
- 1259 Zannoni, N., Leppla, D., Lembo Silveira de Assis, P. I., et al.: Surprising chiral composition  
1260 changes over the Amazon rainforest with height, time and season, *Commun. Earth Environ.*,  
1261 1, 4, <https://doi.org/10.1038/s43247-020-0007-9>, 2020
- 1262 Zannoni, N., Wikelski, M., Gagliardo, A., et al.: Identifying volatile organic compounds used  
1263 for olfactory navigation by homing pigeons, *Sci. Rep.*, 10, 15879,  
1264 <https://doi.org/10.1038/s41598-020-72525-2>, 2020
- 1265 Zhang, B., Jia, Y., Bai, G., Han, H., Yang, W., Xie, W., and Li, L.: Characterizing BVOC  
1266 emissions of common plant species in northern China using real world measurements:  
1267 towards strategic species selection to minimize ozone forming potential of urban greening,  
1268 *Urban For. Urban Green.*, 96, 128341, <https://doi.org/10.1016/j.ufug.2024.128341>, 2024
- 1269